Recent progress in biomass-derived carbon materials used for secondary batteries

doi: https://doi.org/10.1039/D1SE00265A

Recent Progress of Biomass-derived Carbon Materials used for Secondary Batteries

Yun Chen[a], Xiaolin Guo[b*], Anmin Liu [c*], Hongbin Liu[a], Haiding Zhu[c], Yue Zhao[a], and Tingli Ma[ab*]

[a] Graduate School of Life Science and Systems Engineering, Kyushu Institute of Technology 2-4 Hibikino, Wakamatsu, Kitakyushu, Japan
E-mail: tinglima@life.kyutech.ac.jp

[b] College of Materials and Chemistry, China Jiliang University, Hangzhou 310018, P. R. China.
E-mail: guoxiaolin@cjlu.edu.cn

[c] State Key Laboratory of Fine Chemicals, School of Chemical Engineering, Dalian University of Technology, China. E-mail: anmin0127@163.com, liuanmin@dlut.edu.cn

Abstract. With rapid economic development, utilization of energy storage is increasingly important. Carbon materials derived from biomass are widely applied in energy storage systems due to their inexpensive and environmentally friendly. Compared to other advanced anode materials that have been explored, biomass carbon materials have high specific surface areas, adjustable porous structures, and heteroatoms that facilitate ion transfer and diffusion. To date, a series of porous biomass-derived carbon materials prepared through various methods were used as anode electrodes of a secondary battery which greatly promoted their capacities. In this paper, we summarize the morphology and pore structure of biomass-derived materials from different precursors, discuss the electrochemical performance of the secondary batteries (LIBs, SIBs, KIBs and ASSLMBs) equipped with biomass-derived carbon materials including monomers and composites as anode electrodes. Current research challenges along with future prospects for carbon-based electrode materials to improve secondary battery energy storage performance are emphasized.

Introduction

With rapid development of modern industry and human society, the depletion of fossil fuels and related environmental problems are growing evermore serious, and population growth further intensifies the shortage.[1-5] In order to relieve the pressure of energy demand and reduce dependence on fossil fuels, the mainstream approach focuses on the development of sustainable energy technologies, especially electrochemical energy storage systems with the advantages of high efficiency, safety, and flexibility. Currently, chemical power sources have been utilized such as fuel cells, supercapacitors, and secondary batteries. Among these potential sources, secondary batteries have better stability than fuel cells and higher energy density than supercapacitors, and thus firmly occupy the global electrochemical energy storage market[6-8] and are

widely used in portable electronic devices (mobile phones, notebook computers, etc.), electric vehicles, computerized microelectronic mechanical systems, and military equipment (uniforms, gear, drones, etc.). Moreover, the secondary batteries of LIBs, SIBs, and KIBs batteries surpassed those of Ni-MH batteries in both volumetric and gravimetric energy density, as shown in Fig. 1.[9]

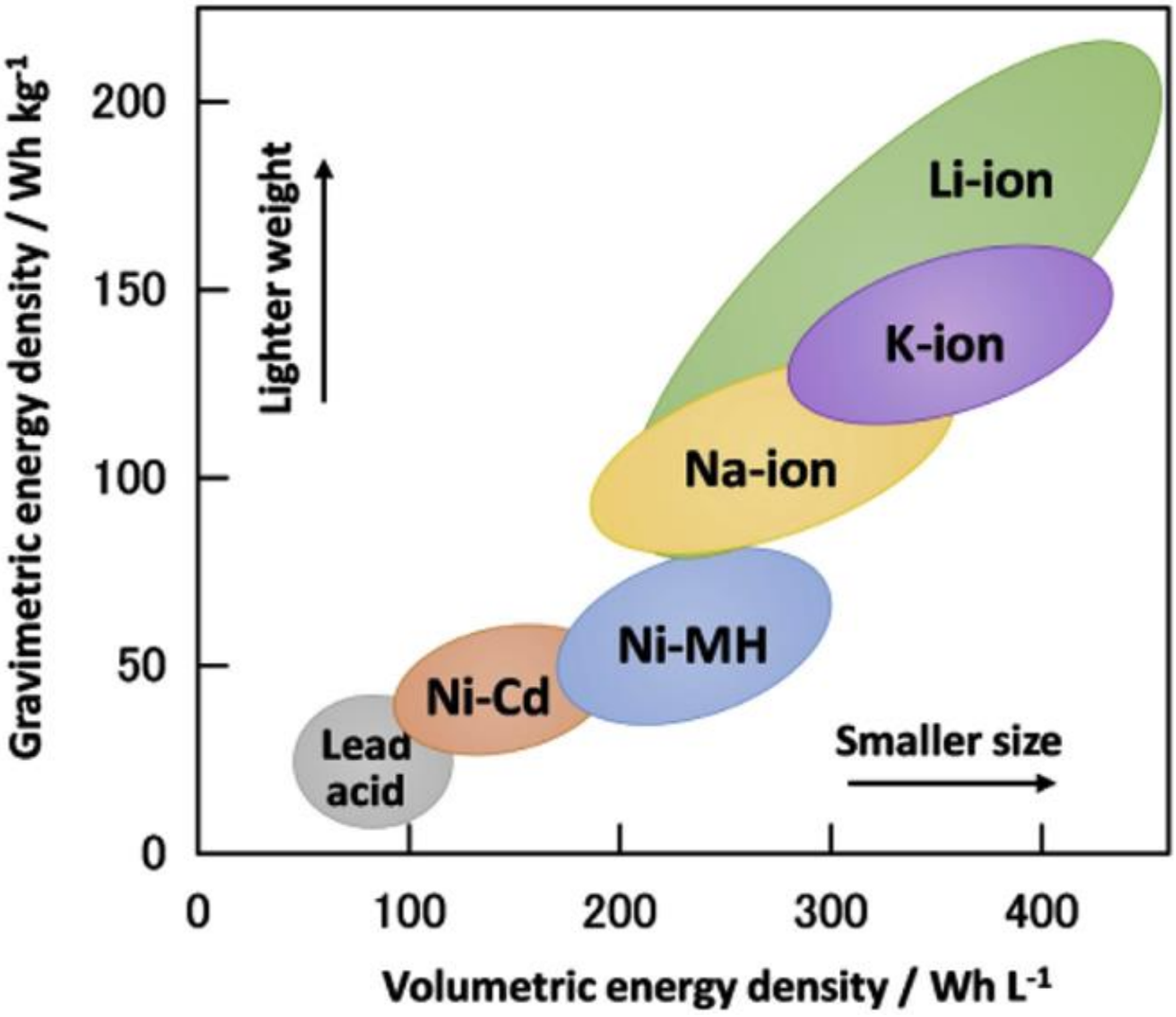

Fig .1 (a) Schematic illustration of the energy density of commercial batteries (Lead acid, Ni-Cd, Ni-MH, LIBs (Li-ion), SIBs (Na-ion), and KIBs (K-ion)). Reproduced with permission from Ref. [9] copyright 2020, Elsevier.

Secondary battery energy storage technology depends on the performance of the electrode material.[10-12] An excellent electrode material should simultaneously satisfy low insertion potential, relatively stable structure, high electronic and ionic conductivity, and high electrolyte compatibility.[13-16] Currently, graphitized carbon and non-graphitized carbon, including hard and soft carbons, are widely studied as primary anode materials. Other titanium-based materials, alloy materials, transition metal oxides, sulfides, and organic precursors are also reported to be high-performance secondary batteries.[17-22] However, to further reduce environmental pollution and promote sustainable energy development, anode materials with abundant resources, low cost, environmentally friendly, and simple to prepare are equally important for large-scale applications of secondary batteries.

Recently, biomass-derived carbon materials have attracted widespread attention as potential materials for anode electrodes due to their superior performance, environmental friendliness, abundance, and renewability. Carbon materials derived from biomass also have special pore structures (including hierarchical porous nanosheets,[23] 3D flatty porous framework,[24] 3D layered porous active,[24-25] and cross-linked porous framework[26]) and chemical element compositions with heteroatom-doping, which make them excellent candidates for the porous carbon material needed for anode electrodes in secondary batteries.[27-30]

Biomass materials from different sources have different chemical components.[31-33] Analysis of the elemental composition shows that biomass carbon materials are rich in carbon compounds and contain large amounts of H, O, N, and the mineral elements of P, S, Ca, K, Mg, Na, and Si.[34-35] Rich in impurities, some types of biomass, such as *Equisetum arvense*,[36-37] rice husk,[38] spinach, wheat bran, and dried dates,[39] containing Si and carbohydrates.[40-43] After acid hydrolysis of the raw materials, it is easy to form a porous structure in situ with a buffer space for volume expansion. Therefore, silicon-carbon materials derived from biomass are commonly investigated as anode electrodes in Lithium-ion batteries.

In this review, biomass precursors were classified by morphology and pore structure for the remains of plant-based, animal-based, and microorganisms. Then, we highlight recent advances in secondary batteries Lithium-ion batteries (LIBs), Sodium-ion batteries (SIBs), Potassium-ion batteries (KIBs)， All-solid-state lithium metal batteries (ASSLMBs) with biomass-derived carbon materials as anode electrodes with respect to composition (carbon or silicon-carbon) and heteroatom-doping (nonmetal atoms or nanoparticles). Finally, we emphasize current challenges and future prospects for carbon-based electrode materials with secondary battery energy storage devices.

Precursors of biomass-derived materials

Plant-biomass materials mainly consist of cellulose, hemicellulose, and lignin—three substances used as biomass carbon sources.[44] Animals-derived biomass mainly includes proteins, fatty acids, and chitin. Chitin-derived carbon nanofibers can be used as anode materials and as battery separators (a barrier between the anode and the cathode).[45-50] The main

components of microorganisms are carbohydrates, protein fibers, and fats, making microorganisms an important source of carbon. Each material requires unique processing according to its unique physical and chemical properties.[51]

Plant-based biomass

Plant-based biomass mainly includes peels, crop straw, leaves, and weeds. Peels function to protect the fruit, and there exists abundant natural pore structures that permit the penetration of water and small-molecule gases, which can act as templates that produce frame pore structure through carbonization. The electrode carbon materials derived from peels usually possess unique multi-layer, multi-structure, and multi-scale morphology. To date, a series of peel-based biomass materials have been studied including banana peels,[52-53] pomelo peels,[54-55] apple peels,[56-57] citrus peels,[58] *Litchi chinensis* peels,[59-60] pistachio peels,[61] coconut shells,[62-64] peanut peels,[65,66] rice husk peels,[67] longan shells,[68] walnut shells,[26] and apricot shells.[69] Mitra et al.[59] prepared porous carbon material by carbonizing litchi peels at 500 ℃ (Fig. 2a). As shown in Figure 2b–e, the average pore diameter is 10μm, evenly distributed. Similarly, Xu et al.[62] reported a biomass-derived carbon material with high surface area composed of coexisting hierarchical pore structures derived from longan shells (Fig. 2f). The thin-walled structures are porous, aiding penetration of electrolytes and reducing resistance of ion migration (Fig. 2g–j).

At present, crop straw is an important biological resource with large output, variety, and wide distribution. Common sources of crop straw include rice straw,[70] wheat straw,[71] corn straw,[72] cotton straw.[73] Other resource-rich biomass materials (leaves and weeds) such as green tea,[74] juncus,[75] leaves,[76] jute fiber,[77] dandelion,[68, 78-79] hemp stems,[80] *E. arvense*, and bamboo leaves have been widely studied as potential electrolytic materials for secondary batteries. As shown in Figure 2k, Ma et al. discovered a weed with high Si content that can be used to derive SiO_x/C materials for use as anode materials in Li-ion batteries.[81] The SEM image illustrates that the surface of the raw weeds contained dense Si with content exceeding 35% in highly-concentrated areas (Fig. 2l–p). When used as an anode in LIBs, it exhibited remarkable capacities (773 mA h g^{-1} at 0.1 A g^{-1}) following 100 cycles and with desirable performance (472 mAh g^{-1} at 1 A g^{-1}). Guo et al.[82] prepared Si/N-doped C/C (SNCC) nanotubes and nano/composite spheres through a simple method using rice husks as the precursor, when used in LIB, it delivered a reversible capacity of 1380 mAh g-1 at 0.5 A g^{-1}.[77]

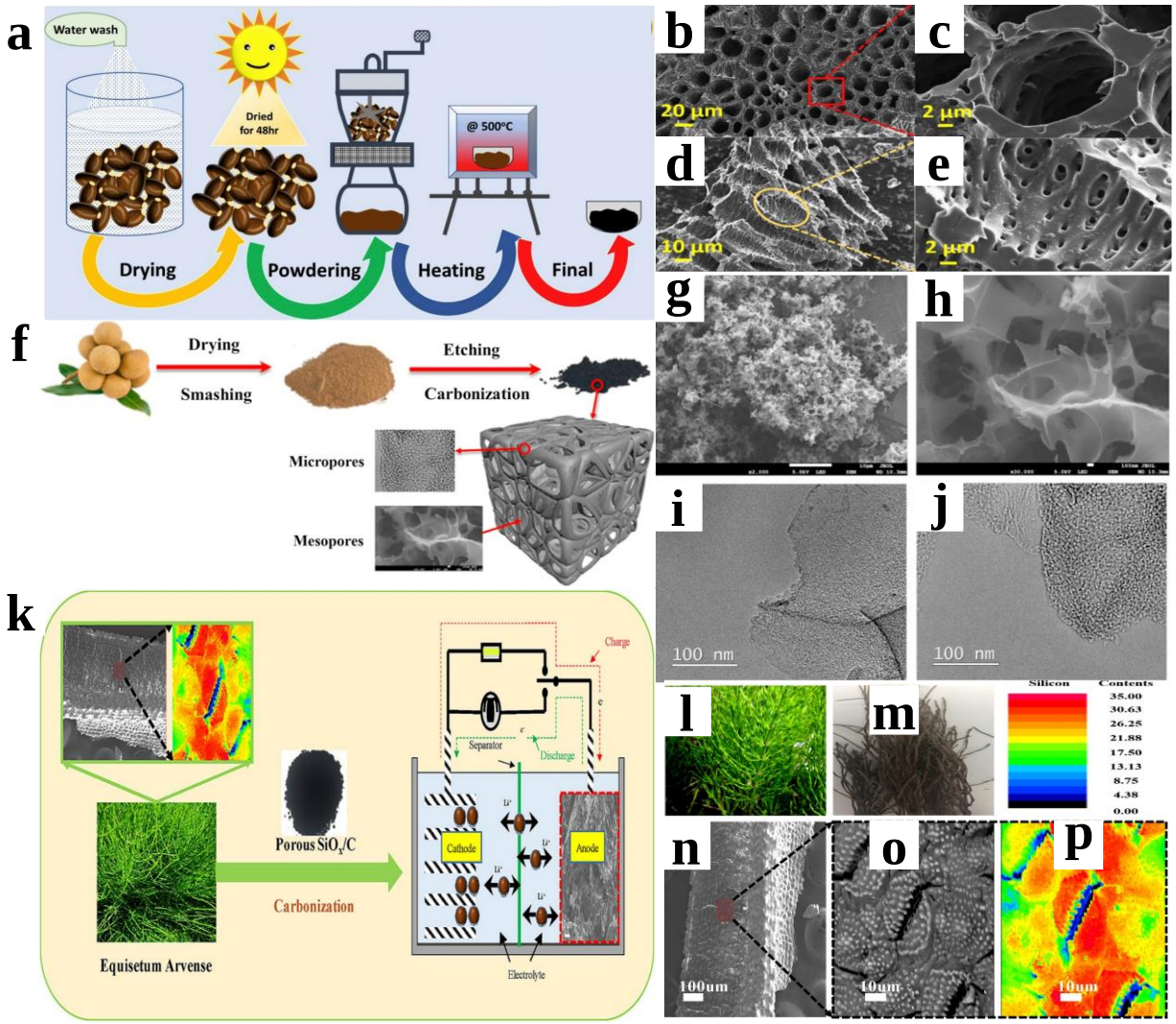

Fig. 2 (a) Schematic of the synthesis of litchi peel sample, (b–e) The FESEM image of the as-prepared litchi peel sample, Reproduced with permission from Ref. [55] Copyright 2019, Elsevier; (f) Schematic of the synthesis of porous carbons from longan shells. (g–j) SEM and TEM of the porous carbons. Reproduced with permission from Ref. [62] Copyright 2018, Elsevier; (k) Schematic of the synthesis of anode material, (l–p) SEM of raw materials of *E. ravens*, Reproduced with permission from Ref. [76] Copyright 2020, Elsevier

Animal-based biomass

Besides lignocellulose in plant-based biomass, the most abundant N-containing organic polymer in nature is chitin which has been proposed as a promising precursor to derive carbon materials doped with N.[83] Gopukumar et al.[84] synthesized a hierarchically macro-meso-micro porous N-doped carbon material from prawn shells by pre-carbonizing the raw material at 300 °C, activating with NaOH, and reheating at 750 °C in an inert Ar atmosphere. Yang and et al.[59] obtained an anode from nanofiber material fabricated by pyrolysis of chitin (Fig. 3a). Atomic Force Microscope (AFM) image shows that

the chitin precursor consisted of nanofibers with the average diameter of 10 to 30 nm (Fig. 3b–c), and the nanofiber morphology was retained after pyrolysis (Fig. 3d–f). The XRD patterns (Fig. 3g) illustrate that the disordered carbon met the theoretical standard for Na ion insertion/extraction at different carbonation temperatures, which facilitated the high capacity and excellent rate capability of Na ion batteries. Qiu et al.[85] synthesized a 2D hierarchical porous carbon using soft pitch as the carbon source and oyster shell as the template and activation agent. The 2D-layered structure surface area is 920 $m^2 \cdot g^{-1}$ and micro/meso-pore size (0.7–9.5 nm) that effectively shortened the solid-state diffusion distance of Li ions in a LIB, which exhibited a high reversible capacity of 1251 $mA \cdot h \cdot g^{-1}$ at $0.1A \cdot g^{-1}$. In addition to the shells of shrimp and crab, human hair[86] and ox horn[87] were utilized as sources of animal-based biomass precursors to synthesize N-doped carbon materials for use as anode material in secondary batteries.

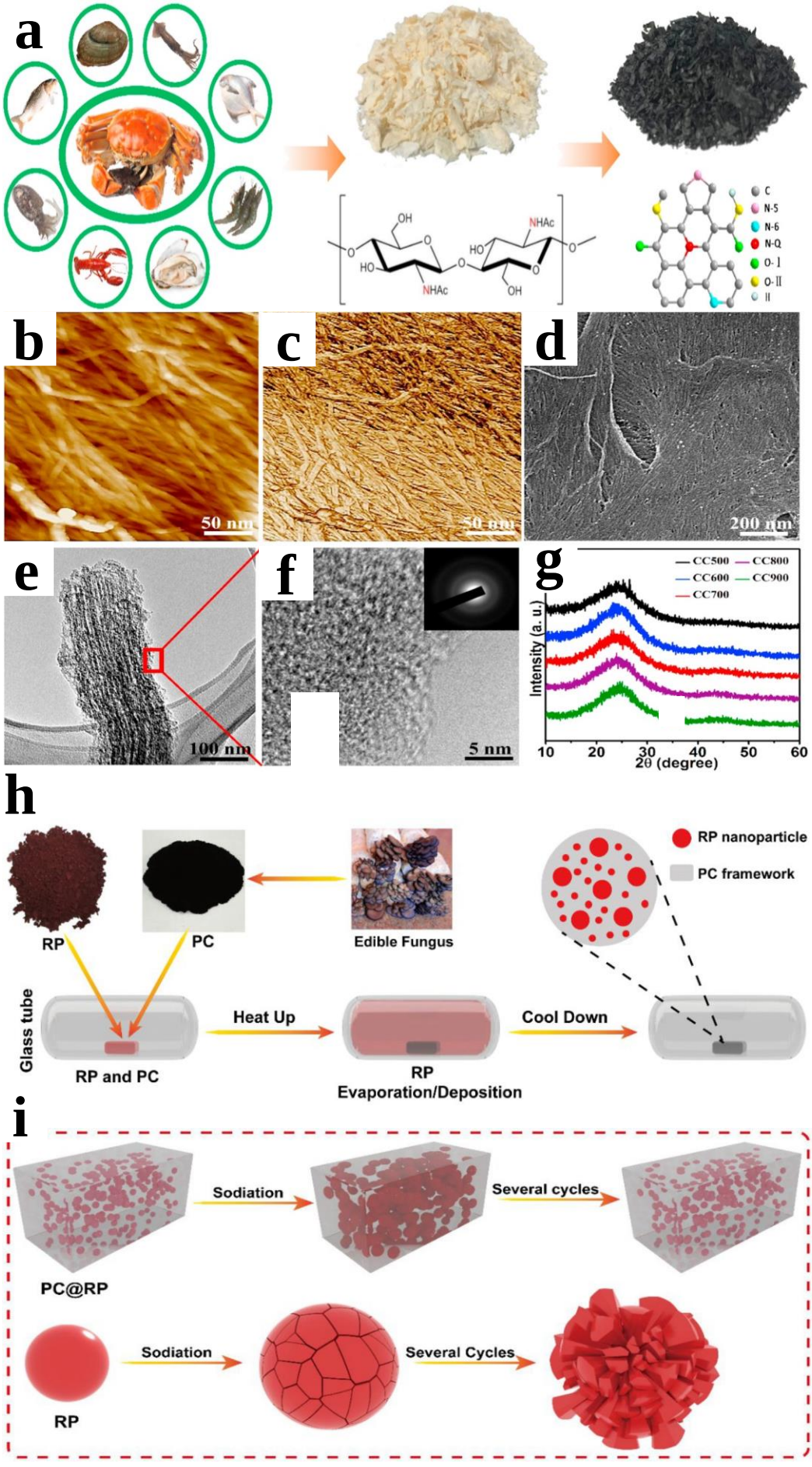
a
OH
NHAc
HO
O
NHAc
HO
OH
C
N-5
N-6
N-Q
O-I
O-II
H
b
50 nm
c
50 nm
d
200 nm
e
100 nm
f
5 nm
g
CC500
CC800
CC600
CC900
CC700
Intensity (a. u.)
10
20
30
40
50
60
2θ (degree)
h
RP
PC
Edible Fungus
RP nanoparticle
PC framework
Glass tube
RP and PC
Heat Up
RP
Evaporation/Deposition
Cool Down
i
PC@RP
Sodiation
Several cycles
RP
Sodiation
Several Cycles

Fig. 3 (a) Schematic the synthesis of carbon nanofibers, (b, c) AFM characterization of NACF, (d–f) SEM characterization of NACF, (g) XRD patterns of the samples (reproduced with permission from Ref. [80] Copyright 2018, Elsevier), (h) Schematic of the synthesized PC@RP porous carbon composite using fungus, (i) slag illustration of the sodiation of PC@RP and RP Particles in SIBs (reproduced with permission from Ref. [85] Copyright 2019, American Chemical Society)

Microorganism-based biomass

In addition to plant-based and animal-based carbon sources, microorganisms are also widely used as the biomass precursor for carbon materials. Penicillium-derived binder-free electrodes,[88] edible fungus slag-derived electrodes,[89] and wild fungus-derived anodes[90] have been studied for use in secondary battery energy storage. Michael Gadd et al.[91] found that electrode materials synthesized through fungal biomineralization of Mn exhibited excellent electrochemical performance and cycle stability, with a capacity retention rate above 90% for 200 cycles in LIBs and proposed this method of synthesis (i.e. use of fungal Mn biomineralization process based on urease-mediated Mn carbonate bioprecipitation) as potential application in the synthesis of biomaterials. Guo et al.[85] synthesized PC @ RP porous carbon composite using fungus slag as the template compounded with red phosphorus (Fig. 3h). The high porosity of fungus slag promoted the positive transmission of Na^+ ions and nano-level red phosphorus, effectively reducing the resistance between electrolytes and electrolytic materials (Fig. 3i). When used in SIBs, the PC @ RP composite maintained high retention rates (87%) after 100 charge/discharge cycles.

Table 1. Electrochemical performance of various biomass-derived anode materials for use in secondary batteries

Materials	**Precursor**	S_{BET} m^2 g^{-1}	**Application**	**Specific Capacity** after 100 cycles	**Ref**
PSDHC-600A	Peanut shell	706.1	LIBs	474 mAh g^{-1} at 1 A g^{-1}	36
BCN	Coconut shell	995.2	LIBs	800 mAh g^{-1} at 0.1 A g^{-1}	66
BPPG	Banana peel	217.3	LIBs	800 mAh g^{-1} at 0.1 A g^{-1}	52
HPC	Honeysuckle	830	LIBs	1215 mAh g^{-1} at 0.1 A g^{-1}	111
N-CNS	soybean	1089	LIBs	550 mAh g^{-1} at 0.5 A g^{-1}	104
FeS/Carbon	Carrageen	852	LIBs	839 mAh g^{-1} at 0.1 A g^{-1}	71
LPG	Loofah	270	LIBs	225 mAh g^{-1} at 0.1 A g^{-1}	158
OHC	ox horn	1300	LIBs	1181 mAh g^{-1} at 0.1 A g^{-1}	86
FeS/Carbon	Carrageen	852	SIBs	227 mAh g^{-1} at 0.1 A g^{-1}	71
BPPG	Banana peel	217.3	SIBs	298 mAh g^{-1} at 0.1 A g^{-1}	52
NP-CNSs	Citrus peels	1167	SIBs	266 mAh g^{-1} at 0.1 A g^{-1}	58
PSDHC-600A	Peanut shell	706.1	SIBs	190 mAh g^{-1} at 0.25 A g^{-1}	36
LPG	Loofah	270	KIBs	150 mAh g^{-1} at 0.1 A g^{-1}	158
CNM	prawn shell	336	LIBs	740 mAh g^{-1} at 0.1 A g^{-1}	82
CNM	prawn shell	336	SIBs	325 mAh g^{-1} at 0.1 A g^{-1}	82
OPDHC-A	orange peel	1272	SIBs	156 mAh g^{-1} at 0.5 A g^{-1}	92

Note: PSDHC-600A (porous hard carbons-600A); BCN (boron carbonitride); BPPG (Banana peel pseudographite); HPC (hierarchical porous carbon); N-CNS (ultra-thin carbon nanosheets); LPG (loofah-derived pseudo-graphite); OHC (ox horn derived carbon); NP-CNSs (nanoporous carbon nanosheets); PSC (prawn shell derived carbon); OPDHC-A (orange peel derived hard carbon)

Applications in LIB anode electrode

LIBs have become the first choice for green batteries in the 21st century and the most promising research object for scholars and scientists.[92] Generally, graphite is the most representative anode material in LIBs because of its low Li intercalation potential which prevents deposition of Li metal dendrites and improves security; however, the theoretical capacity of a graphite anode is only 372 $mA \cdot h \cdot g^{-1}$, which is needs to be elevated for LIB applications.[93] The theoretical capacity of Si is 4200 mAh g^{-1} when fully intercalated with Li, with an actual capacity of 4000 mAh g^{-1}, which is 10 times the capacity of graphite.[94] These intrinsically-desirable molecular structures and architectures are favorable for energy storage and transport toward a sustainable energy economy. Large volume expansion (360% for $Li_{4.4}Si$) and poor electrical conductivity hinder application of Si-based anode materials in LIBs. One of the most effective strategies is the use of Si-C compounds which have high capacity, good conductivity, and good stability.[95] Anode materials doped with atoms of N, P, and S can expand the surface area, provide more reaction sites, and enhance conductivity, which is beneficial to the absorption and transfer of ions during the charging process. According to the way in which the heteroatoms are introduced, the biomass-derived carbon can be divided into intrinsically-doped carbon and extrinsically-doped carbon.[96]

Biomass-derived carbon

Non-doped carbon.

In general, carbon materials derived directly from pyrolysis of biomass requires further treatment with an activation reagent such as KOH to increase surface area and porosity. Specifically, as the biomass-derived carbon substrate is etched by the KOH, micropores and mesopores form during the redox reaction process and the water vapor contributes to the fabrication of pores during activation. Moreover, K ions (K^+), as the activated intermediate, can be inserted into the carbon skeleton to further expand the spacing of crystal planes.[97-98] Tian et al.[65] studied peanut shell-derived carbon anodes carbonized at 600 ℃ with and without KOH activation (PSDHC-600 A and PSDHC-600). Compared with PSDHC-600, PSDHC-600A shows richer pore structure (Fig. 4a–d) and greater surface area (from 375.2 to 706.1 $m^2 \cdot g^{-1}$, Fig. 4e). For LIB applications, the reversible capacity increased from 314 to 474 $mA \cdot h \cdot g^{-1}$ at 1 $A \cdot g^{-1}$ after 400 cycles for PSDHC-600 and PSDHC-600A, respectively (Fig. 4f), and retained its capacity at 310 $mA \cdot h \cdot g^{-1}$ after 10,000 cycles at 5 $A \cdot g^{-1}$. Kim et al.[74] synthesized a carbon anode derived from discarded green tea with a spherical nanostructure and average diameter of 30 nm. The cyclic voltammetry curves illustrated that a solid electrolyte interface (SEI) formed on the surface of the anode during the first cycle, which enhanced the reversible capacity to 498 $mA \cdot h \cdot g^{-1}$ after 100 cycles when applied in LIBs.

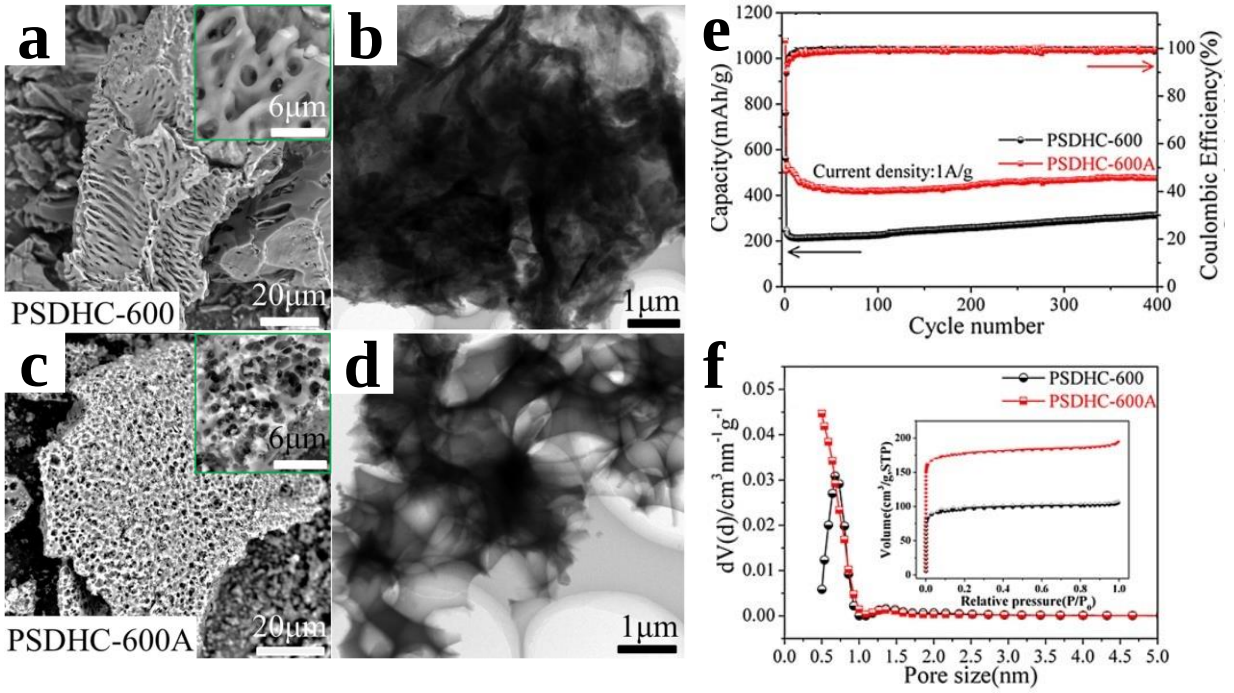

Fig. 4 (a, c) SEM, (b, d) TEM of the sample, (e) BET of the sample, (f) electrochemical performances of PSDHC-600 and PSDHC-600A for LIB applications. Reproduced with permission from Ref. [59] Copyright 2015, Elsevier.

In addition to potassium hydroxide,[59] zinc chloride,[99] sodium hydroxide,[100] potassium carbonate,[78] sulfuric acid,[79] and phosphoric acid[80] were also used as activators for carbon materials derived from biomass. Sun et al.[99] derived anode materials with high specific surface area of 1191.30 $m^2 g^{-1}$ from rice husks using a $ZnCl_2$ activation method. When used for LIB applications, this material delivered a reversible capacity of 1105 mAh g^{-1} at 0.1 A g^{-1} after 360 cycles. Jusef Hassoun et al.[101] used different activators to obtain AC-H (H_3PO_4) and AC-K (KOH) derived from cherry pits and found that AC-H had higher specific surface area (1662 $m^2 g^{-1}$) compared to AC-K (1171 $m^2 g^{-1}$), and that AC-H had better electrochemical performance at low rates, while AC-K exhibited excellent performance at high rates.

Carbon doped with nonmetal atoms/single atoms.

Doping of carbon with heteroatoms forms defects and active sites, and enhances the electrical conductivity of the anode material, which in turn improves the electrochemical performance in LIBs.[102] How the heteroatoms are introduced to can be classified as intrinsic doping and extrinsic doping.[103-104] Intrinsic doping means that the precursor contains heteroatoms, and thus the heteroatoms are more likely retained in the skeleton of the carbon material during the carbonization cracking process. High stability and low cost are obvious advantages of the intrinsic doping method; however, the content of the heteroatom is easily limited by the precursor, causing inadequate doping. For extrinsic doping, the substance

containing the heteroatom reacts with the biomass precursor to obtain the target product without strict limitations on the amount of dopant. Among the different dopant atoms, N atoms are the most widely used dopants to introduce defects to biomass-derived electrode materials.[81,82] Doping with N atoms can strengthen the wettability of biomass-based electrode materials and improve the migration rate of ions, which improve the performance of the anode material. To date, carbon materials with high N content have been prepared, including ultra-thin carbon nanosheets derived from soybean milk,[105] nitrogen doped porous carbon materials derived from duckweed,[106] and nitrogen doped porous carbon from *Ginkgo biloba* as precursors.[107]

Xiao et al.[87] prepared N-rich porous carbon materials by pyrolysis of ox horns activated with KOH, and the specific surface area of the material increased from 10 to 1300 $m^2 g^{-1}$. Moreover, XPS spectra showed that C, O, and N were the main elements in the derived material and the N content reached 5.5%. The high N content indicates that the generation of defects and enhanced the conductivity of the carbon material and the electrochemical performance in LIBs with a specific capacity of 1181 mAh g^{-1} at 0.1 A g^{-1} and 304 mAh g^{-1} at 5 A g^{-1}. Xiao et al.[71] reported a porous N-rich material (HPNC) with a surface area of 916.0 $m^2 g^{-1}$. The hierarchically-porous HPNC was derived from wheat straw, which was carbonized under an Ar atmosphere at 700 °C and activated by potassium hydroxide with a mass ratio of 3:1. The crude protein in the wheat straw precursor contributed to the high N content in HPNC and was used as the anode material for the LIBs, in which the reversible cycling capacity of HPNC achieved 1470 mAh g^{-1} with 0.1 C and 344 mAh g^{-1} at 50 C. In addition, Kim et al.[108] synthesized a N-doped carbon material derived from shaddock peel using a carbamide-induced N-doping procedure and attributed the expansion of interlayer spacing and optimization of porous structure during formation of the C-N bonds.

Carbon doped with multiple atoms.

In addition to N, doping with S atoms also provides more active sites and enhances the conductivity of electrode materials,[109-111] therefore, doping with multiple nonmetal atoms has been widely applied to modify biomass-derived carbon materials. Xiang et al.[112] reported on electrode materials (HPC) co-doped with S and N directly derived from the biomass of honeysuckle. Elemental mapping and SEM images demonstrate that S and N are evenly distributed in carbon-based material with a 3D porous hierarchical structure. For LIB applications, the reversible capacity of HPC was 1215 mAh g^{-1} at 0.1 A g^{-1} and 370 mAh g^{-1} at 20 A g^{-1} after 100 cycles. Excellent electrochemical performance was attributed to the multi-level porous nanostructure and the introduction of heteroatoms, which reduced the diffusion resistance between the electrolyte and electrode material and facilitated the transport of Li ions. Similarly, Ciucci et al.[113] developed P and N dual atom-doped carbon material (PNCC) from egg yolk. When used as a half-cell electrode material, its shows a reversible capacity of 770 mAh g^{-1} at 0.5 A g^{-1} after 100 cycles. Wang et al.[114] reported that a carbon-based material

doped with S, N, and O (NOSDCA-3) derived from algal-derived carrageen. The SEM and TEM images showed the sponge-like interconnected porous structure of NOSDCA-3. The XPS showed that the elemental content of C, N, O, and S are 85.87%, 1.65%, 7.69%, and 4.79%, respectively. When tested as LIB anodes, a reversible capacity of 839 mAh g^{-1} at 0.1 A g^{-1} and a capacity of 228 mAh g^{-1} at 10 A g^{-1} were obtained.

Carbon composed with TMO/TMS.

Transition metal oxides and sulfides (TMO/TMS) have been widely studied due to their high theoretical capacity based on the reaction: TMO (TMS) + $2Li^+$ + 2e- ↔ Li_2O (Li_2S) + TM; however, this reaction is accompanied by a drastic change in volume during charging and discharging. Composed with the conductive supporting substrates is a strategy to relive the structural change and maintain the stability of TMO/TMS. Biomass-derived carbon materials are suitable as buffer for anode materials and many researchers have synthesized X/biomass-derived carbon composites (where X represents $Li_4Ti_5O_{12}$,[115] $NiCo_2O_4$,[55] $ZnMn_2O_4$,[116] FeS_2,[117] $Co_{1-x}S$,[118] and Co_3O_4[119]) to improve the stability and reversible capacity in LIBs.

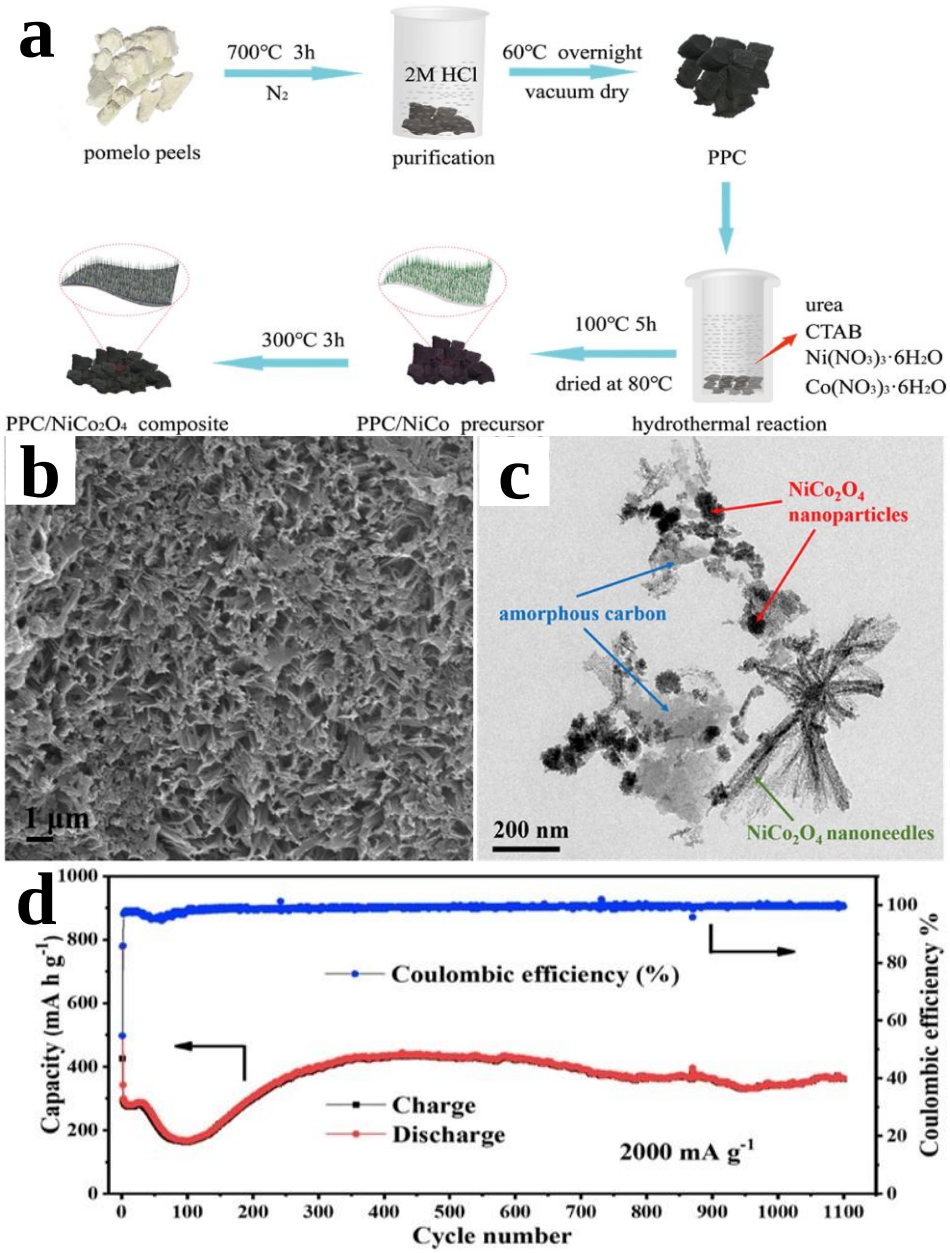

Fig. 5 (a) Scheme of synthesis of PPC/$NiCo_2O_4$ composite, (b) SEM, (c) TEM of the PPC/$NiCo_2O_4$ composite, (d) cycling performance of PPC/$NiCo_2O_4$ composite. Reproduced with permission from Ref. [51] Copyright 2020, Elsevier

Liang et al.[55] synthesized carbon material derived from pomelo peels (PPC) and composited it with $NiCo_2O_4$ nanoparticles to obtain PPC/$NiCo_2O_4$ (Fig. 5a). The SEM images show a very thin layer of $NiCo_2O_4$ covering the PPC surface following hydrothermal and heat treatments (Fig. 5b, c). As used in LIBs, PPC/$NiCo_2O_4$ shows a reversible capacity of 473.7 mAh g^{-1} at 0.5 A g^{-1} after 210 cycles, and 363 mAh g^{-1} at 2 A g^{-1} after 1100 cycles. Zhang et al.[116] reported a pine needle-

derived $ZnMn_2O_4$/PNC composite prepared by the hydrothermal method. When used as anode material in LIBs, this composite showed excellent storage performance and cycle stability with a reversible capacity of 1000 mAh g^{-1} at 0.2 C and 727 mAh g^{-1} at 2.0 C after 500 cycles, respectively. Lee et al.[120] fabricated a Sn/C composite extracted from microalgal biomass. For LIBs, this composite exhibited a reversible capacity of 511.7 mAh g^{-1} at 200 mA g^{-1} after 300 cycles.

Biomass-derived silicon-based/carbon composite

Si/C composite

Lithium-ion batteries with anodes made from Si have a maximum theoretical capacity of 4200 mAh g^{-1} and a lower discharge potential than Li/Li^+,[121] which is considered to strong potential prospects as an LIB electrode material. However, Si-based materials have poor electronic conductivity and high volume deformation (about 300%) during charge and discharge.[122] Compositing Si nanoparticles with carbon materials is an effective strategy to improve cycle stability, which provides a larger buffer space for Si/C material, alleviates agglomeration of Si nanoparticles, and improves the conductivity of Si to a certain extent.[123-124] Some kinds of biomass, such as reeds, chaff, weeds, and bamboo, contain both SiO_2 and lots of carbohydrates. After acid hydrolysis of the raw materials, it is easy to form a porous structure in situ to provide a buffer space for volume expansion and have been widely investigated as anodes in LIBs. Yu et al.[125] synthesized a 3D porous Si/C anode material using reed plants as the source of Si. The reed precursor was calcined and reduced with Mg to obtain porous silica; then compounded with glucose to obtain porous Si/C material (yield of Si ~ 4%, Fig. 6a). The TEM images show an even layer of carbon covering the surface of the porous 3D Si structure, which improved the conductivity of anode and enhanced cycle stability with a retention capacity of 420 mA h g^{-1} at 10 C after 4000 cycles. Yu et al.[126] prepared a porous 3D Si from bamboo charcoal composited with polyacrylonitrile to prepare a Si@N/C material. For LIB applications, a reversible capacity of 603 mAh g^{-1} at 0.2 A g^{-1} and a maximum capacity of 360 mAh g^{-1} at 1.6 A g^{-1} after 120 cycles. The excellent electrochemical performance demonstrates that N-doped carbon can improve the conductivity of the Si/N-doped carbon composite anode material and accommodate the volume change better during cycling (Fig. 6b). Guo et al.[82] prepared a Si/N-doped carbon/carbon nanotube spheres anode material using rice husk as the Li-ion precursor. In this work, they used electrospray ionization method and carbonization to obtain nanospheres with microstructures.

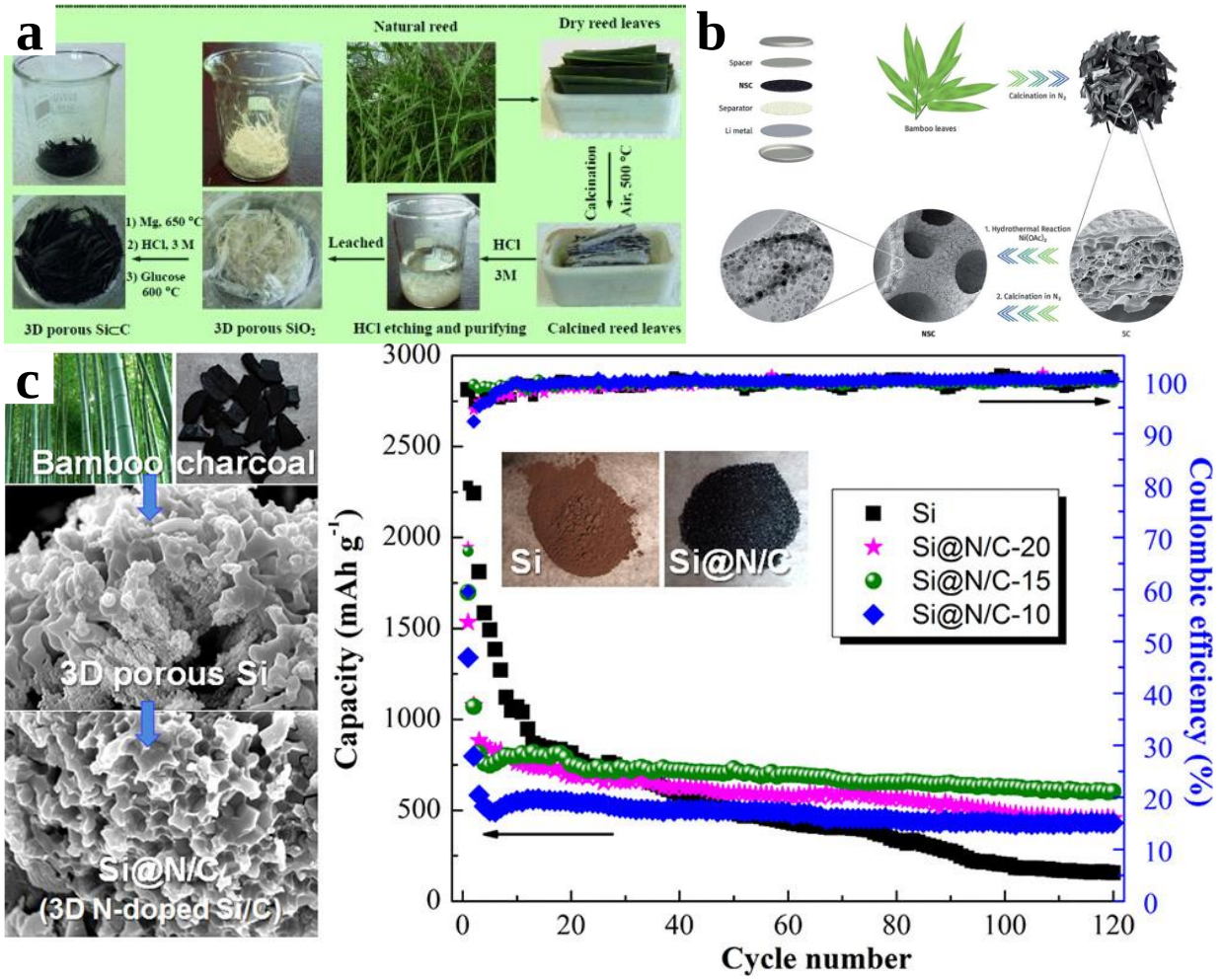

Fig. 6 (a) Schematic of synthesis of porous 3D Si/C anode (reproduced with permission from Ref. [120] Copyright 2015, Wiley), (b) schematic of synthesis of the NSC anode (reproduced with permission from Ref. [126] Copyright 2020, Elsevier), (c) schematic of synthesis of Porous Si@N/C Composites (reproduced with permission from Ref. [121] Copyright 2018, Elsevier)

SiO_x/C composite

Since Si-based materials have problems caused by volume expansion and poor cycle stability, SiO_x with smaller volumes of expansion (<150%) present an alternative to popular anode materials used in LIBs.[127-128] Gao et al.[129] prepared SiO_x/C nanoparticles (10–50 nm) using rice husks, which contain abundant C and 20 wt% SiO_x, as the precursor. SiO_x/C nanoparticles were obtained in a two-step carbonization process at 900 °C under an Ar/H atmosphere. The reduced atmosphere facilitated formation of low valence Si in SiO_x/C nanoparticles, which delivered a maximum reversible

capacity of 600 mAh g^{-1} after 100 cycles at 0.1 A g^{-1}. Similarly, using $ZnCl_2$ as the activating agent to carbonize rice husks, Sun et al.[130] fabricated a porous C/SiO_2 composite with surface area 1191.30 m^2 g^{-1}. High surface area increased the contact area between C/SiO_2 anode material and the electrolyte thereby promoting Li^+ diffusion at their interface and contributing to an excellent reversible capacity of 1105 mAh g^{-1} at 0.1 A g^{-1} after 360 cycles. Pang et al.[131] developed highly stable ternary Ni/SiO_x/N-doped carbon (NSC) anode material derived from bamboo. SiO_x/N-doped carbon (SC) framework provided sufficient space to buffer volume expansion during lithiation. The uniform Ni nanoparticles (NPs) on the SC matrix restricted the formation of cracks, reduced volume expansion, and thus improved the electrical conductivity of SiO_x. The electrode exhibited a discharge capacity of 864.6 mAh g^{-1} at 0.2 A g^{-1} and 289.8 mAh g^{-1} at 10 A g^{-1} after 70 cycles in LIBs. Ma et al.[74] prepared Sn/$SnSiO_{x+2}$@C-650 anode material (Fig. 7a) using a one-pot treatment of biomass (*Fatsia japonica*), the glass phase of SiO_{x+2}, and Sn nanoparticles. The Sn/$SnSiO_{x+2}$@C-650 delivered a maximum reversible specific capacity of 919 mAh g^{-1} at a current density of 0.2 mA g^{-1} after 100 cycles (Fig. 7c). After 100 cycles, the electrode thickness increased from the original 32.3 μm (Fig. 7b) to 39.1 μm (Fig. 7c), while the volume expansion was controlled within 20%.

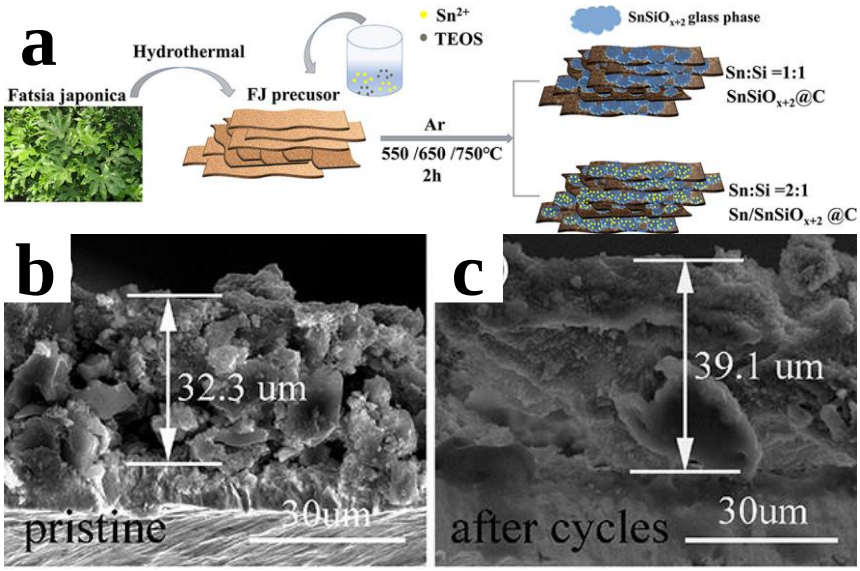

Fig. 7 (a) Schematic of synthesis of biomass-derived carbon framework, and cross-sectional SEM images of the Sn/SnSiOx+2@C-650 electrode (b) before and (c) after 100 cycles (with permission from Ref. [69] Copyright 2019, American Chemical Society)

Applications in SIB anode electrodes

Given the high price of Li, the element Na, which is in the same group as Li, has attracted attention in its potential application as a secondary battery because of its lower price and abundance. The energy storage mechanisms in the SIBs and LIBs are roughly the same with respect to the insertion and extraction of ions on the electrode material. However, the graphite that is widely used in LIBs cannot meet the requirements for anode material in SIBs because Na ions have a larger radius (1.07 Å) than lithium ions (0.76 Å).[132-134] Biomass carbon is produced by the carbonization of natural biomass, and most natural biomass is composed of hard carbon materials which are difficult to graphitize.[135] To date, various biochars derived from biomass have been prepared and used as anode materials for SIBs.[75, 136-138]

Non-doped carbon

Shi et al.[139] obtained straw-derived carbon material for anodes (RS-x samples) by pre-processing and carbonization at different temperatures (i.e. 900, 1100, 1300, and 1500 ^{o}C). As shown in the SEM images (Fig. 8a–d), the RS-x samples were made of micron-grade block, and the surface was covered with a layer of nanospheres. The SIB electrode material of the RS-1100 sample had the highest reversible capacity of 291.1 mAh g^{-1} after 200 cycles at 0.4 C (Fig. 8e–f) due to the proper interlayer spacing in this sample, which was conducive to the insertion and extraction of Na ions. The storage mechanism of Na ions was revealed for the RS-x electrode on which Na ions adsorbed onto the micropores and defects in the sloping region (≥0.1 V), while in the plateau region (<0.1 V), Na ions were inserted into the graphite-like nanolayer (Fig. 8g). As the pyrolysis temperature rose, the interlayer spacing and adsorption area declined although the number of layers and the value of La increased. Similarly, Pol et al.[140] obtained SIB anode materials derived from pistachio shells that carbonized at 700 to 1500 ^{o}C under an Ar atmosphere. The Raman spectroscopy revealed that the larger D-Raman peak and G-Raman peak I_D/I_G ratio along with increased temperature of carbonization revealed the formation of sp^2 rings and the transformation of sp^3 carbon. Compared to other samples, the sample carbonized at 1000 ^{o}C (surface area = 760.9 m^2 g^{-1}) delivered the highest reversible capacity of 225 mAh g^{-1} at 10 mA g^{-1}.

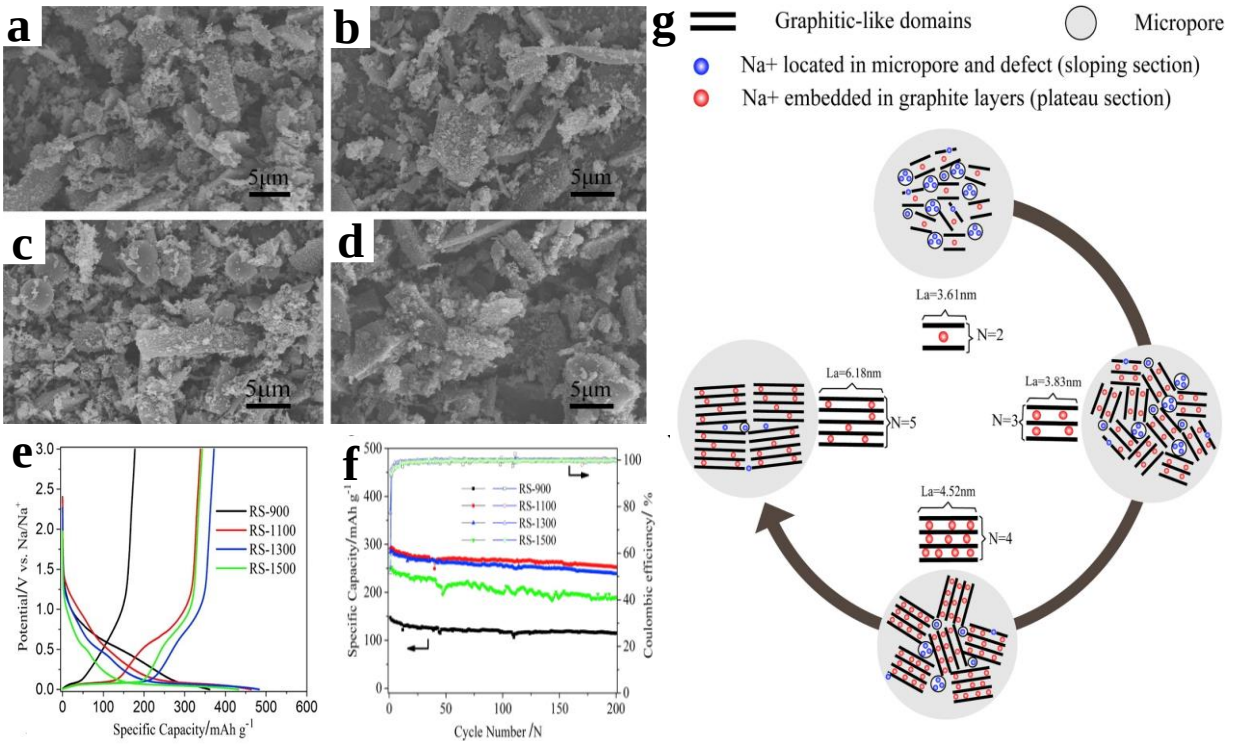

Fig. 8 SEM image of RS-x. (a) RS-900, (b) RS-1100, (c) RS-1300, (d) RS-1500, (e) discharge/charge curves,(f) cyclic performance, (g) mechanism of RS-x electrodes for sodium storage (reproduced with permission from Ref. [131] Copyright 2018, Elsevier)

Carbon doping with nonmetal atoms

Single atom

Introducing dopant atoms into the carbon sp^2 lattice to replace carbon atoms could form more defects, increase electronic conductivity and the number of active sites of the heteroatom-doped carbon.[141-142] In general, the dopant atoms B, N,[143] Fl,[144] S,[145] and P[146] are common in SIB applications. Ci et al.[147] derived porous N-doped carbon materials from egg yolk through carbonization at 650 ℃ and washing with NaOH and HCl to remove impurities. The XPS spectra revealed that the N in porous carbon can be divided into quaternary N and hexagonal pyridinic N with a total carbon content of 4.6%. Also, heteroatom doping and low carbonization temperatures cause high disorder of carbon (I_D/I_G ratio was about 0.94). Nitrogen-doped porous carbon anode material used in SIB applications delivered a reversible capacity of 208 mAh g^{-1} at 0.1 A g^{-1}. Sun et al.[148] prepared a series of 3D layered S-doped biomass materials—S-OS, S-GP, S-ES, and S-LL derived from onion skin, garlic peel, elm samara, and lotus leaf, respectively (Fig. 9a–d). The SEM images show that these biomass precursors have similar 3D frameworks of parallel flakes (Fig. 9e–h), which were well-preserved after the S-doping carbonization process (Fig. 9i–l). For SIB applications, the S-OS, S-GP, S-ES, and S-LL precursors delivered

specific capacities of 178.4, 155.6, 145.7, 176.1 mA h g^{-1}, respectively, at 5 A g^{-1}, demonstrating the excellent performance of these S-doped carbon materials (Fig. 9m–p).

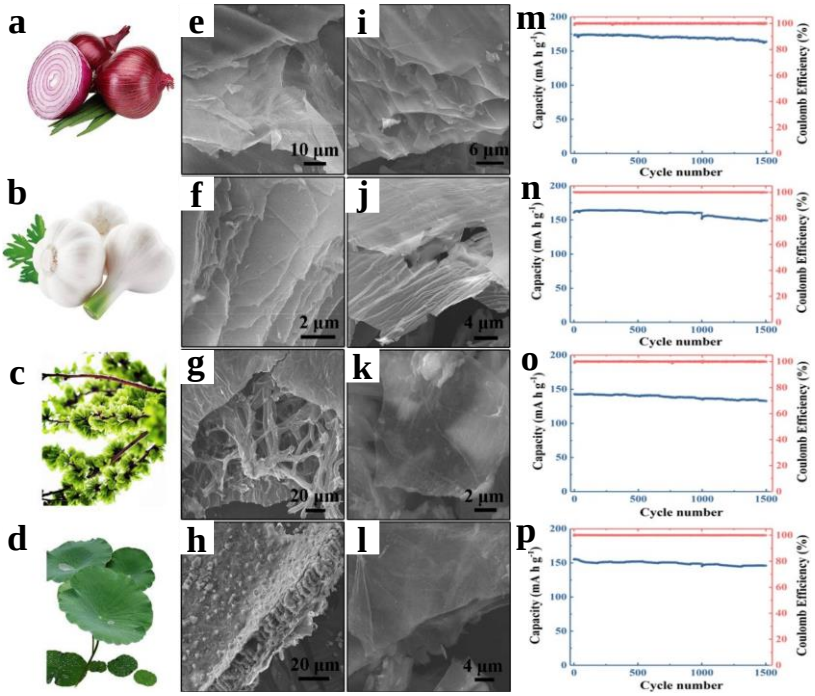

Fig. 9 (a–d) Digital photographs; (e–h) SEM images of onion skin, garlic peel, elm samara, and lotus leaf; (i–l) SEM images of the S-OS, S-GP, S-ES, S-LL samples; (m–p) electrochemical performance of the S-OS, S-GP, S-ES, and S-LL samples (reproduced with permission from Ref. [140] Copyright 2019, Elsevier)

Multiple atoms

In general, carbon materials doped with multiple heteroatoms including B-N,[149] N-S, and N-P[150] have been applied as anode material in SIBs. Zhang et al.[151] synthesized N and S dual-doping carbon through hydrolyzation of bean shells. Broad beans are rich in resources and contain a series of heteroatoms including O, N, and S, which are naturally excellent precursors for heteroatom-doped carbon materials. These electrodes exhibit a high initial discharge capacity of 466.3 mAh g^{-1} at 0.2 A g^{-1} and outstanding cycle performance, with great potential for application in SIBs.

Carbon composed of nanoparticles

Yang et al.[152] prepared highly-porous FeS/carbon fibers (FeS/CFs) for use as anode material with an Fe-carrageenan composite as the precursor. During preparation of the Fe-carrageenan fiber (Fig. 10a), Fe^{+} can promote the formation of a double helix structure and strengthen the aggregation of different double helix, which is conducive to long-distance

cross-linking. The FeS nanoparticles are formed in situ by interacting with the S-containing group of carrageenans and uniformly embedded in the unique 1D porous carbon fibrous matrix (Fig. 10b–d).

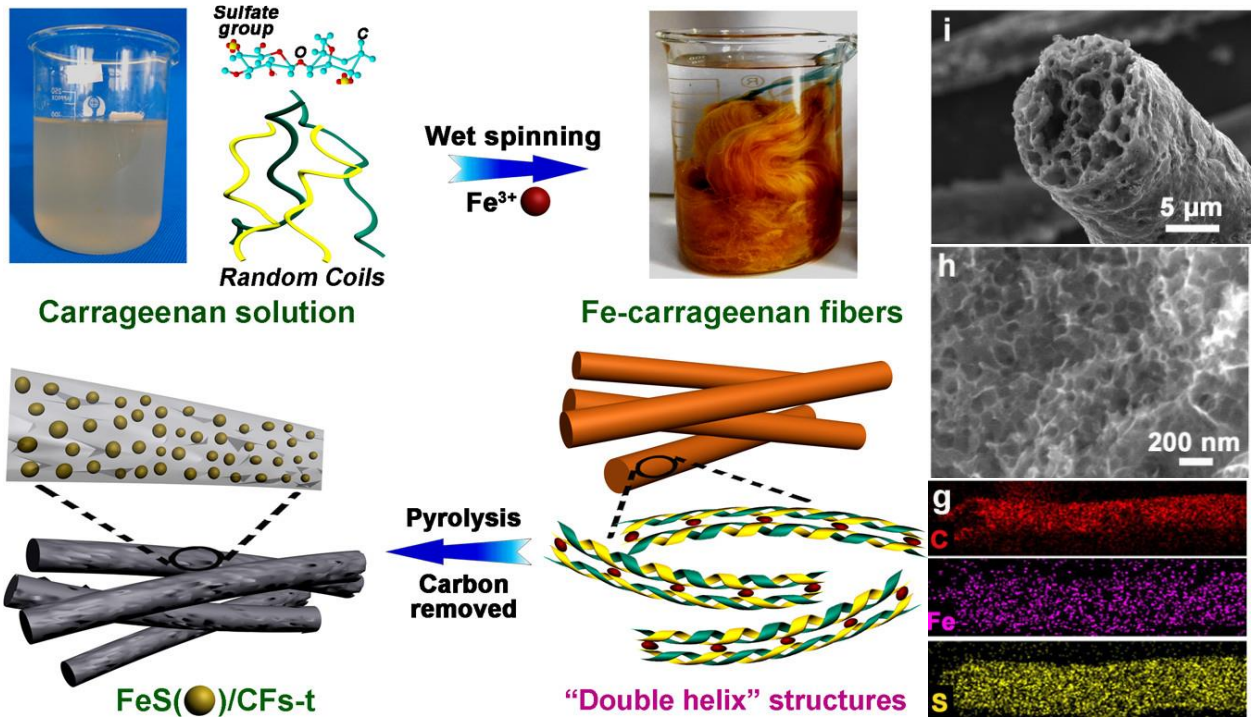

Fig. 10 (a–d) Digital photographs; (e–h) SEM images of onion skin, garlic peel, elm samara, and lotus leaf; (i–l) SEM images the of the S-OS, S-GP, S-ES, and S-LL samples; (m–p) electrochemical performances of S-OS, S-GP, S-ES, and S-LL samples (reproduced with permission from Ref. [145] Copyright 2018, Elsevier Copyright 2018, American Chemical Society)

After pyrolysis in an Ar atmosphere, the Fe-carrageenan fibers decompose to FeS/CFs, and porous FeS/CFs were obtained by calcining at 600 °C in a CO_2 atmosphere. The composite material delivered a high capacity of 283 mAh g^{-1} at 1 A g^{-1} and rate of 247 mAh g^{-1} at 5 A g^{-1} after 400 cycles.

Dan et al.[153] prepared hierarchical iron phosphides/biomass carbon materials using the electrodeposition method to composite the iron phosphide with the carbon biomass derived from magnolia leaf. The porous carbon enhanced the electrical conductivity and reduced the mechanical stress due to the iron phosphides. The nanosheet structure of the phosphides/biomass carbon increased the specific surface area, provided more active sites, and shortened the ion diffusion channel. The electrode delivered a reversible capacity of 500.9 mAh g^{-1} at a current density of 0.05 A g^{-1} and 197 mAh g^{-1} at 0.5 A g^{-1} after 100 cycles. The Sb_2O_4/C composite prepared by Dutta[154] used Indian blackberry seeds as the carbon precursor and found that disordered carbon created a massive network of space, which increased conductivity, provided

a buffer for volume expansion which in turn benefitted stability during the charge/discharge process, and exhibited a high reversible capacity of 236 mAh g^{-1} at a current density of 1 A g^{-1}after 125 cycles.

Applications in potassium ion batteries and all solid-state lithium battery

Potassium ion batteries

Currently, LIBs are one of the most commonly used energy storage systems;[155-156] however, the shortage of Li resources create a need for alternatives. In addition to Na ions, K-ion batteries (KIBs) are of interest because of the abundant resources and appropriate oxidation-reduction potential of K ions.[157-158] Lu et al.[159] prepared potato biomass porous carbon (PBPC) approximately 10 nm in diameter (Fig. 11a). When used as anode material for KIBs, the PBPC exhibited excellent electrochemical performance, with a reversible capacity of 248 mAh g^{-1} at 0.1 A g^{-1} and a coulomb efficiency exceeding 99% (Fig. 11b). Similarly, Yao et al.[160] found that *Ganoderma lucidum* spores—a traditional Chinese medicinal material with abundant protein, amino acids, and vitamins—have a natural hollow cage-like structure and a double wall. Through simple carbonization, a porous carbon material shows a specific surface area of 104.4 m^2 g^{-1} and stable mesopore/macropore structure was obtained (Fig. 11c–f). For KIB applications, this porous carbon material anode material exhibited a reversible capacity of 163.8 mAh g^{-1} after 100 cycles at of 0.2 A g^{-1} (Fig. 11g).

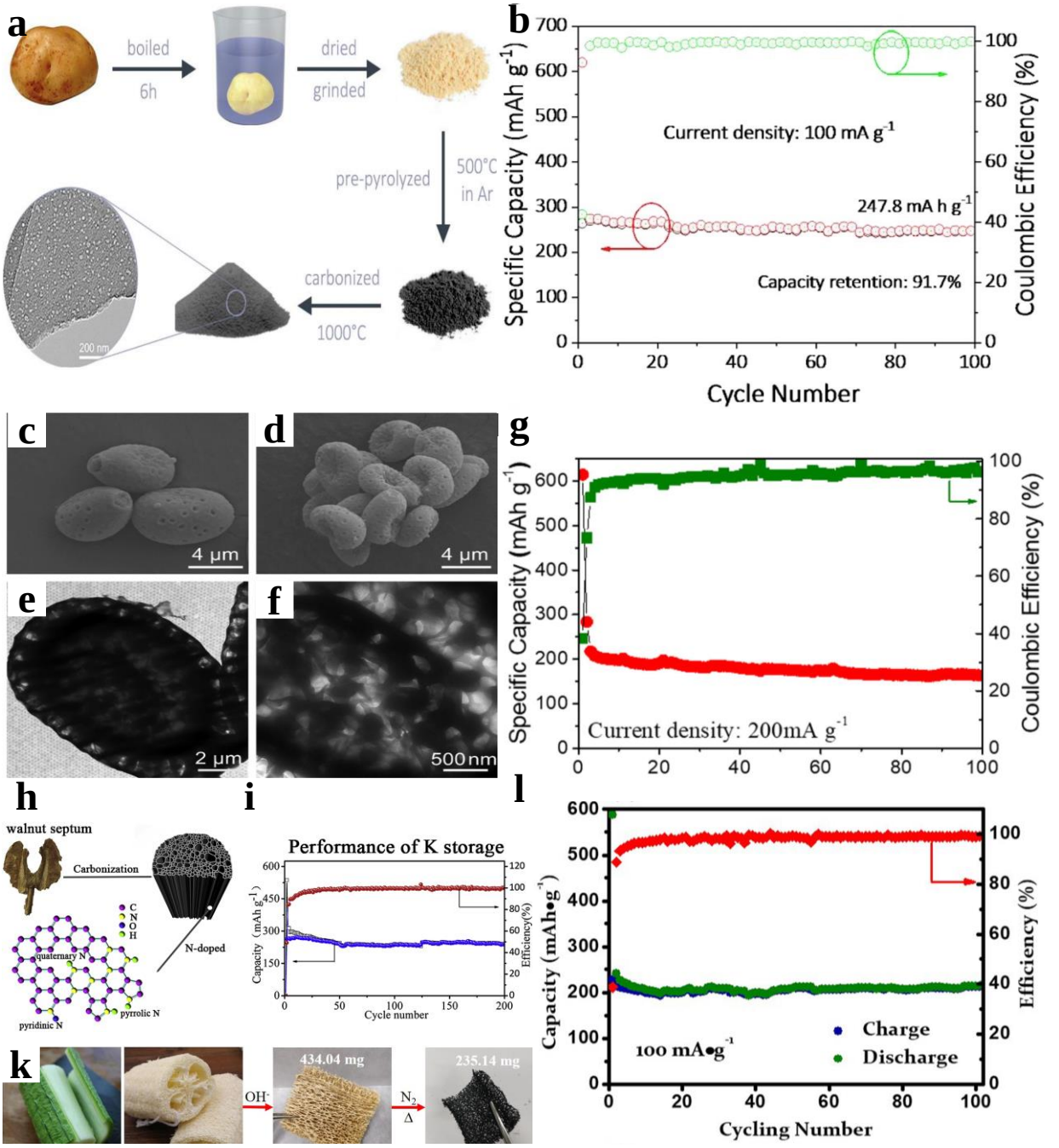

Fig. 11 (a) Schematic illustration of the potato biomass porous carbon (PBPC) derived from potato. (b) Discharge and charge capacity and coulombic efficiency of PBPC-1000 at 0.1 A g^{-1} (reprinted with permission from Ref. [151], Copyright 2018, Elsevier). (c) SEM image of untreated *Ganoderma lucidum* spore. (d) SEM image of CPC. (e, f) TEM image of CPC (reprinted with permission from Ref. [152], Copyright 2020, Elsevier). (h) Schematic illustration of the synthesis of N-doped walnut septum. (i) Charge and discharge at of 100 mA g^{-1} (reprinted with permission from Ref.

[153], Copyright 2019, Elsevier). (k) Schematic illustration of the synthesis of Loofah-derived carbon. (l) Capacity of *Luffa*-derived carbon (reprinted with permission from Ref. [154], Copyright 2019, Elsevier)

Guo et al.[161] obtained N-doped hierarchical porous carbon (NHPC) materials from walnut septum (Fig. 11h). The layered structure, large interlayer spacing, and numerous active sites contributed to the excellent electrochemical performance of NHPC as an anode material in KIBs with a reversible capacity of 242.5 mAh g^{-1} after 200 cycles at 0.1 A g^{-1} (Fig. 11i). Niu et al.[162] derived a hard carbon material (pseudo-graphite) from a *Luffa* by one-step pyrolysis (Fig. 11k). The graphite-like units on a micron scale and near-surface defects on a larger scale contributed to the dual-ion storage mechanism of the Loofah-derived carbon material, and achieved good electrochemical performance as both anode material in both LIBs and KIBs (Fig. 11).

All-solid-state lithium metal batteries

To date, the safety issues and limited cycle life limits the commercialization of lithium metal batteries. Use of newer nonflammable solid electrolytes in place of traditional organic flammable electrolytes can reduce the risk of fire and explosion. Considering the defects of the anode materials, an ideal frame material is required for constructing the novel solid multi-level structure lithium metal electrode. Therefore, adopting a multi-level structure inside the electrode is an effective way to enhance the interface contact and improve the performance of the solid-state lithium metal battery.[163-165] Inspired by the multi-level structure of diatomite, Yu et al.[166] prepared a multi-level Li metal solid composite anode with a stable structure and without dendritic growths (Fig. 12). They transformed natural diatomite (Fig. 12a) into a silicon framework (Fig. 12b) with a multi-level pore structure using the magnesium thermal reduction method. The multi-level structure of the Si framework was mixed with molten lithium and stirred to prepare the lithium-silicon composite powder (Fig.12c). Next, polyethylene oxide polymer solid electrolyte (PEO-SPE) was used to modify the surface of the lithium-silicon powder. Finally, the powder was cold-pressed into a mold to form a composite lithium metal negative electrode (PEO-DLSL) with a multi-level structure. In the PEO-DLSL, the lithium metal is embedded in the pore structure of the PEO-SPE-modified $Li_{4.4}Si$ frame, thereby increasing its contact area with the electrolyte, which is beneficial in obtaining a uniform Li ion flow and maintaining the electrode structure "Completeness." As a result, at high current density (>0.5 mA cm^{-2}), the multi-level structure of the lithium metal composite anode derived from diatomite achieved uniform deposition and extraction of lithium metal, which effectively inhibited lithium dendrites. With PEO-SPE as the solid electrolyte, the PEO-DLSL symmetric battery can be cycled for more than 1000 h without short circuiting during the lithium extraction/deposition test, and the polarization voltage can be maintained below 100 mV. Researchers further investigated the performance of PEO-DLSL in all solid-state lithium metal batteries (PEO-SPE is a solid electrolyte with lithium iron phosphate as the positive electrode). The PEO-DLSL-based solid-state lithium metal battery showed superior

cycle stability (500 cycles can be cycled at a rate of 0.5 C, and the capacity decay rate of 0.04 % per cycle), which is an advantage over the solid lithium metal battery using flat lithium foil with a short circuit after 75 cycles (Fig. 12d).

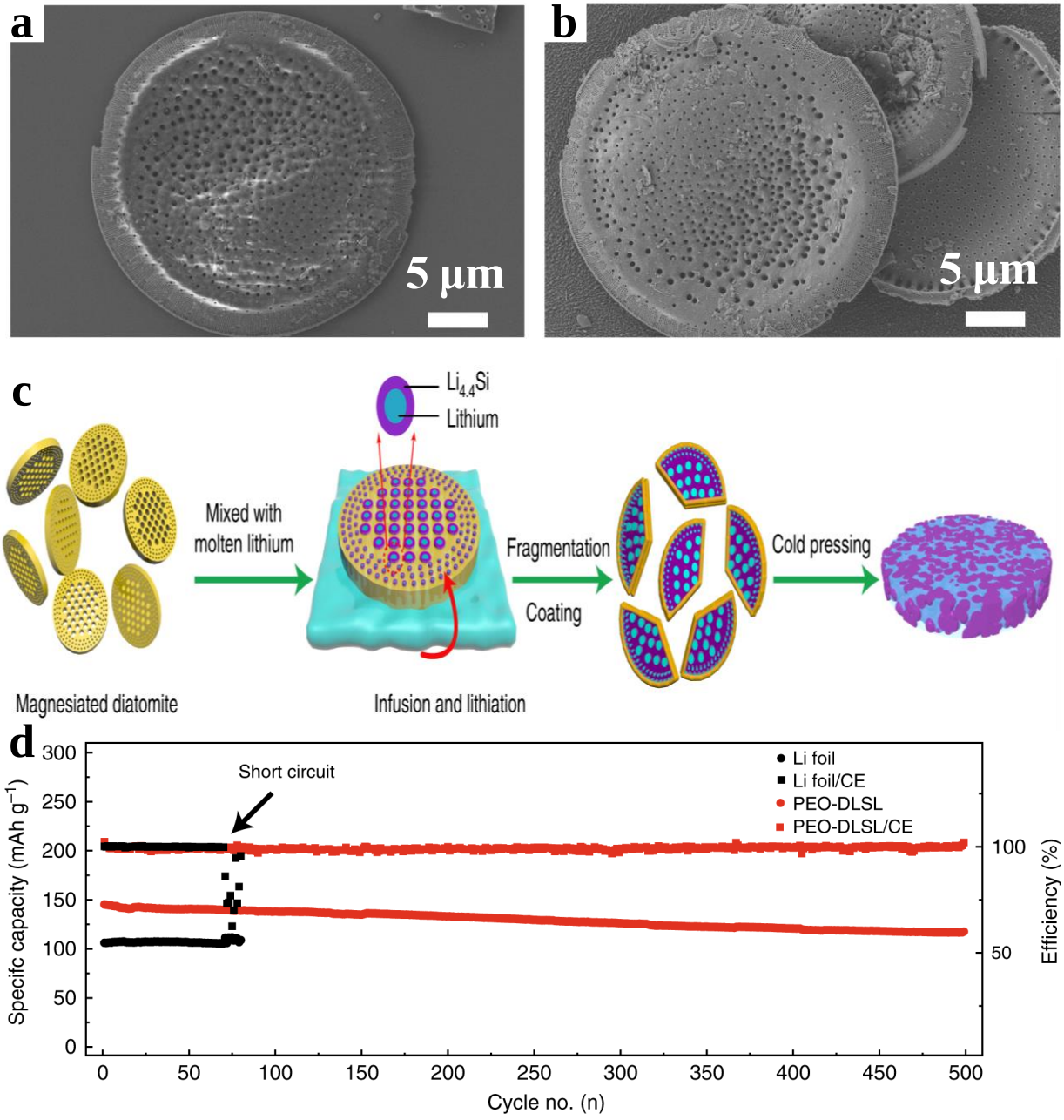

Fig. 12 (a–b) SEM images of pristine diatomite framework (DF) and DF-Si, respectively. (c) The fabrication process of PEO-DLSL. (d) Long-term cycling performance of batteries at a current density of 0.5 C. Reprinted with permission from Ref. [158], Copyright 2019, Springer.

Conclusions and Perspectives

Nowadays, biomass-derived anode is widely studied as electrode materials as new energy storage devices due to their large specific surface area, stable structure and excellent electrical conductivity etc. The demand for green and sustainable energy storage materials provokes the development of low-cost and eco-friendly anode materials for the secondary batteries. Biomass, as a rich, cheap and easily available renewable resource, provides sufficient raw materials for preparing porous carbon materials. In this review, we summarized the diversity of structural characteristics of common biomass precursors for carbon materials to be used in secondary batteries to store energy and introduced the application of biomass-derived carbon anode materials in LIBs, SIBs, KIBs, and All-solid-state lithium metal batteries, with respect to composition and heteroatom-doping. By classifying the biomass materials according to the source of their precursor, the material composition and structural characteristics provide a reference for further design and application of biomass materials in the field of secondary batteries. The carbon materials doped with nonmetal elements improve electrical conductivity and facilitate transmission of electrons, therefore electrochemical performance of carbon-based anode materials can be enhanced. Carbon materials doped with metal elements also increase the discharge specific capacity, energy power, and energy density because the heteroatoms narrow the band gap and thereby enhance conductivity.

Although materials derived from biomass show great potential as anode material in secondary batteries, there are issues that limit further application. First, biomass-derived carbon has various porous structures and morphology, and thus it is not easy control the quality or quantity of material needed for mass production. The best way to scale up production for biomass-derived carbon materials from the laboratory stage to industrial application needs further exploration, and future research should be directed towards the development of structurally-controlled biomass-based carbon materials to achieve sustainable development strategies. In addition, Biomass-derived carbon material has low first coulomb efficiency and poor stability, which restrict their large-scale development seriously. And hopefully, the development and application of heteroatom doping or compounding with other compounds can be an effective solution to the problem. Furthermore, Biomass-derived carbon material needs to choose some lower-cost precursors that are not restricted by geographical restrictions and seasonal restrictions for the development from laboratory to industrialization.

In addition to secondary batteries, biomass materials have also been fully studied in other fields such as supercapacitors, fuel cells, Wastewater treatment, gas adsorption and catalyst， biomedicine, sensor device. Currently, with the continuous innovation of new energy technology, researchers are constantly increasing the research passion on low-cost and pollution-free biomass materials. We believe that biomass materials will definitely be a very shining star in this energy revolution.

Acknowledgements

This work was supported by the Grant-in-Aid for Scientific Research (KAKENHI) program, Japan (B, Grant Number 19H02818), and the National Natural Science Foundation of China (Grant No. 51772039 and 51972293).

References

1. Chou, S.; Yu, Y., Next Generation Batteries: Aim for the Future. *Advanced Energy Materials* **2017,** *7* (24), 1703223.
2. Delmas, C., Sodium and Sodium-Ion Batteries: 50 Years of Research. *Advanced Energy Materials* **2018,** *8* (17), 1703137.
3. Deng, J.; Luo, W.-B.; Chou, S.-L.; Liu, H.-K.; Dou, S.-X., Sodium-Ion Batteries: From Academic Research to Practical Commercialization. *Advanced Energy Materials* **2018,** *8* (4), 1701428.
4. Sun, N.; Guan, Z.; Liu, Y.; Cao, Y.; Zhu, Q.; Liu, H.; Wang, Z.; Zhang, P.; Xu, B., Extended "Adsorption–Insertion" Model: A New Insight into the Sodium Storage Mechanism of Hard Carbons. *Advanced Energy Materials* **2019,** *9* (32), 1901351.
5. Xu, F.; Qiu, Y.; Han, H.; Jiang, G.; Zhao, R.; Zhang, E.; Li, H.; Wang, H.; Kaskel, S., Manipulation of carbon framework from the microporous to nonporous via a mechanical-assisted treatment for structure-oriented energy storage. *Carbon* **2020,** *159*, 140-148.
6. Jian, Z.; Xing, Z.; Bommier, C.; Li, Z.; Ji, X., Hard Carbon Microspheres: Potassium-Ion Anode Versus Sodium-Ion Anode. *Advanced Energy Materials* **2016,** *6* (3), 1501874.
7. Jian, Z.; Hwang, S.; Li, Z.; Hernandez, A. S.; Wang, X.; Xing, Z.; Su, D.; Ji, X., Hard-Soft Composite Carbon as a Long-Cycling and High-Rate Anode for Potassium-Ion Batteries. *Advanced Functional Materials* **2017,** *27* (26), 1700324.
8. Luo, W.; Wan, J.; Ozdemir, B.; Bao, W.; Chen, Y.; Dai, J.; Lin, H.; Xu, Y.; Gu, F.; Barone, V.; Hu, L., Potassium Ion Batteries with Graphitic Materials. *Nano letters* **2015,** *15* (11), 7671-7.
9. El Kharbachi, A.; Zavorotynska, O.; Latroche, M.; Cuevas, F.; Yartys, V.; Fichtner, M., Exploits, advances and challenges benefiting beyond Li-ion battery technologies. *Journal of Alloys and Compounds* **2020,** *817*, 153261.
10. Wang, Y.; Fu, X.; Zheng, M.; Zhong, W. H.; Cao, G., Strategies for Building Robust Traffic Networks in Advanced Energy Storage Devices: A Focus on Composite Electrodes. *Advanced materials* **2019,** *31* (6), e1804204.
11. Mahmood, N.; Tang, T.; Hou, Y., Nanostructured Anode Materials for Lithium Ion Batteries: Progress, Challenge and Perspective. *Advanced Energy Materials* **2016,** *6* (17), 1600374.
12. Goodenough, J. B.; Park, K. S., The Li-ion rechargeable battery: a perspective. *J Am Chem Soc* **2013,** *135* (4), 1167-76.
13. Zhong S, Liu H, Wei D, et al. Long-aspect-ratio N-rich carbon nanotubes as anode material for sodium and lithium ion batteries[J]. Chemical Engineering Journal, 2020, 395: 125054.
14. Iordache, A.; Delhorbe, V.; Bardet, M.; Dubois, L.; Gutel, T.; Picard, L., Perylene-Based All-Organic Redox Battery with Excellent Cycling Stability. *ACS applied materials & interfaces* **2016,** *8* (35), 22762-7.
15. Zhang, X.; Jin, L.; Dai, X.; Chen, G.; Liu, G., Two-Dimensional GaN: An Excellent Electrode Material Providing Fast Ion Diffusion and High Storage Capacity for Li-Ion and Na-Ion Batteries. *ACS applied materials & interfaces* **2018,** *10* (45), 38978-38984.

16. Saeed, G.; Kumar, S.; Kim, N. H.; Lee, J. H., Fabrication of 3D graphene-CNTs/α-MoO3 hybrid film as an advance electrode material for asymmetric supercapacitor with excellent energy density and cycling life. *Chemical Engineering Journal* **2018,** *352*, 268-276.
17. Fang, S.; Bresser, D.; Passerini, S., Transition Metal Oxide Anodes for Electrochemical Energy Storage in Lithium - and Sodium - Ion Batteries. *Advanced Energy Materials* **2019,** *10* (1), 1902485.
18. Li, Q.; Li, L.; Wu, P.; Xu, N.; Wang, L.; Li, M.; Dai, A.; Amine, K.; Mai, L.; Lu, J., Silica Restricting the Sulfur Volatilization of Nickel Sulfide for High - Performance Lithium - Ion Batteries. *Advanced Energy Materials* **2019,** *9* (43), 1901153.
19. Li, H.; Wu, P.; Xiao, Y.; Shao, M.; Shen, Y.; Fan, Y.; Chen, H.; Xie, R.; Zhang, W.; Li, S.; Wu, J.; Fu, Y.; Zheng, B.; Zhang, W.; Huo, F., Metal-Organic Frameworks as Metal Ion Precursors for the Synthesis of Nanocomposites for Lithium-Ion Batteries. *Angewandte Chemie* **2020,** *59* (12), 4763-4769.
20. Cao, Y.; Zhang, T.; Zhong, X.; Zhai, T.; Li, H., A safe, convenient liquid phase pre-sodiation method for titanium-based SIB materials. *Chem Commun (Camb)* **2019,** *55* (98), 14761-14764.
21. Fedotov, S. S.; Luchinin, N. D.; Aksyonov, D. A.; Morozov, A. V.; Ryazantsev, S. V.; Gaboardi, M.; Plaisier, J. R.; Stevenson, K. J.; Abakumov, A. M.; Antipov, E. V., Titanium-based potassium-ion battery positive electrode with extraordinarily high redox potential. *Nature communications* **2020,** *11* (1), 1484.
22. Song, K.; Liu, C.; Mi, L.; Chou, S.; Chen, W.; Shen, C., Recent Progress on the Alloy-Based Anode for Sodium-Ion Batteries and Potassium-Ion Batteries. *Small* **2019**, e1903194.
23. Li, Y.; Wang, G.; Wei, T.; Fan, Z.; Yan, P., Nitrogen and sulfur co-doped porous carbon nanosheets derived from willow catkin for supercapacitors. *Nano Energy* **2016,** *19*, 165-175.
24. Fu, H.; Xu, Z.; Li, R.; Guan, W.; Yao, K.; Huang, J.; Yang, J.; Shen, X., Network Carbon with Macropores from Apple Pomace for Stable and High Areal Capacity of Sodium Storage. *ACS Sustainable Chemistry & Engineering* **2018,** *6* (11), 14751-14758.
25. Chen, D.; Li, L.; Xi, Y.; Li, J.; Lu, M.; Cao, J.; Han, W., Self-assembly of biomass microfibers into 3D layer-stacking hierarchical porous carbon for high performance supercapacitors. *Electrochimica Acta* **2018,** *286*, 264-270.
26. Tao, L.; Huang, Y.; Zheng, Y.; Yang, X.; Liu, C.; Di, M.; Larpkiattaworn, S.; Nimlos, M. R.; Zheng, Z., Porous carbon nanofiber derived from a waste biomass as anode material in lithium-ion batteries. *Journal of the Taiwan Institute of Chemical Engineers* **2019,** *95*, 217-226.
27. Long, W.; Fang, B.; Ignaszak, A.; Wu, Z.; Wang, Y. J.; Wilkinson, D., Biomass-derived nanostructured carbons and their composites as anode materials for lithium ion batteries. *Chemical Society reviews* **2017,** *46* (23), 7176-7190.
28. Wang, J.; Nie, P.; Ding, B.; Dong, S.; Hao, X.; Dou, H.; Zhang, X., Biomass derived carbon for energy storage devices. *Journal of Materials Chemistry A* **2017,** *5* (6), 2411-2428.
29. Gaddam, R. R.; Yang, D.; Narayan, R.; Raju, K.; Kumar, N. A.; Zhao, X. S., Biomass derived carbon nanoparticle as anodes for high performance sodium and lithium ion batteries. *Nano Energy* **2016,** *26*, 346-352.
30. Liu, T.; Kavian, R.; Chen, Z.; Cruz, S. S.; Noda, S.; Lee, S. W., Biomass-derived carbonaceous positive electrodes for sustainable lithium-ion storage. *Nanoscale* **2016,** *8* (6), 3671-7.
31. Cherubini, F.; Strømman, A. H., Chemicals from lignocellulosic biomass: opportunities, perspectives, and potential of biorefinery systems. *Biofuels, Bioproducts and Biorefining* **2011,** *5* (5), 548-561.
32. Manyà, J. J.; Azuara, M.; Manso, J. A., Biochar production through slow pyrolysis of different biomass materials: Seeking the best operating conditions. *Biomass and Bioenergy* **2018,** *117*, 115-123.
33. Watkins, D.; Nuruddin, M.; Hosur, M.; Tcherbi-Narteh, A.; Jeelani, S., Extraction and characterization of lignin from different biomass resources. *Journal of Materials Research and Technology* **2015,** *4* (1), 26-
32. Vassilev S V, Baxter D, Andersen L K, et al. An overview of the chemical composition of biomass[J]. Fuel, 2010, 89(5): 913-933.
34. Vassilev, S. V.; Baxter, D.; Andersen, L. K.; Vassileva, C. G., An overview of the chemical composition of biomass. *Fuel* **2010,** *89* (5), 913-933.

35. Fang, J.; Guo, D.; Kang, C.; Wan, S.; Li, S.; Fu, L.; Liu, G.; Liu, Q., Enhanced hetero‐elements doping content in biomass waste‐derived carbon for high performance supercapacitor. *International Journal of Energy Research* **2019**.
36. Pallag A, Filip G A, Olteanu D, et al. Equisetum arvense L. extract induces antibacterial activity and modulates oxidative stress, inflammation, and apoptosis in endothelial vascular cells exposed to hyperosmotic stress[J]. Oxidative medicine and cellular longevity, 2018, 2018.
37. Vivancos, J.; Deshmukh, R.; Gregoire, C.; Remus-Borel, W.; Belzile, F.; Belanger, R. R., Identification and characterization of silicon efflux transporters in horsetail (Equisetum arvense). *J Plant Physiol* **2016,** *200*, 82-9.
38. Hu L, He Z, Zhang S. Sustainable use of rice husk ash in cement-based materials: Environmental evaluation and performance improvement[J]. Journal of Cleaner Production, 2020, 264: 121744.
39. Meena, V. D.; Dotaniya, M. L.; Coumar, V.; Rajendiran, S.; Ajay; Kundu, S.; Subba Rao, A., A Case for Silicon Fertilization to Improve Crop Yields in Tropical Soils. *Proceedings of the National Academy of Sciences, India Section B: Biological Sciences* **2013,** *84* (3), 505-518.
40. Bakhat, H. F.; Bibi, N.; Zia, Z.; Abbas, S.; Hammad, H. M.; Fahad, S.; Ashraf, M. R.; Shah, G. M.; Rabbani, F.; Saeed, S., Silicon mitigates biotic stresses in crop plants: A review. *Crop Protection* **2018,** *104*, 21-34.
41. Luyckx, M.; Hausman, J. F.; Lutts, S.; Guerriero, G., Silicon and Plants: Current Knowledge and Technological Perspectives. *Front Plant Sci* **2017,** *8*, 411.
42. Chen, D.; Chen, D.; Xue, R.; Long, J.; Lin, X.; Lin, Y.; Jia, L.; Zeng, R.; Song, Y., Effects of boron, silicon and their interactions on cadmium accumulation and toxicity in rice plants. *J Hazard Mater* **2019,** *367*, 447-455.
43. Zhu, Y. X.; Gong, H. J.; Yin, J. L., Role of Silicon in Mediating Salt Tolerance in Plants: A Review. *Plants (Basel)* **2019,** *8* (6).
44. Laurichesse, S.; Avérous, L., Chemical modification of lignins: Towards biobased polymers. *Progress in Polymer Science* **2014,** *39* (7), 1266-1290.
45. Fu, M.; Chen, W.; Ding, J.; Zhu, X.; Liu, Q., Biomass waste derived multi-hierarchical porous carbon combined with CoFe2O4 as advanced electrode materials for supercapacitors. *Journal of Alloys and Compounds* **2019,** *782*, 952-960.
46. Lei, S.; Chen, L.; Zhou, W.; Deng, P.; Liu, Y.; Fei, L.; Lu, W.; Xiao, Y.; Cheng, B., Tetra-heteroatom self-doped carbon nanosheets derived from silkworm excrement for high-performance supercapacitors. *Journal of Power Sources* **2018,** *379*, 74-83.
47. Niu, J.; Shao, R.; Liang, J.; Dou, M.; Li, Z.; Huang, Y.; Wang, F., Biomass-derived mesopore-dominant porous carbons with large specific surface area and high defect density as high performance electrode materials for Li-ion batteries and supercapacitors. *Nano Energy* **2017,** *36*, 322-330.
48. Ren, M.; Lu, X.; Chai, Y.; Zhou, X.; Ren, J.; Zheng, Q.; Lin, D., A three-dimensional conductive cross-linked all-carbon network hybrid as a sulfur host for high performance lithium-sulfur batteries. *Journal of colloid and interface science* **2019,** *552*, 91-100.
49. Wang, D.; Xu, Z.; Lian, Y.; Ban, C.; Zhang, H., Nitrogen self-doped porous carbon with layered structure derived from porcine bladders for high-performance supercapacitors. *Journal of colloid and interface science* **2019,** *542*, 400-409.
50. Xu, Z.; Li, Y.; Li, D.; Wang, D.; Zhao, J.; Wang, Z.; Banis, M. N.; Hu, Y.; Zhang, H., N-enriched multilayered porous carbon derived from natural casings for high-performance supercapacitors. *Applied Surface Science* **2018,** *444*, 661-671.
51. Arroyo, J.; Farkas, V.; Sanz, A. B.; Cabib, E., 'Strengthening the fungal cell wall through chitin-glucan cross-links: effects on morphogenesis and cell integrity'. *Cell Microbiol* **2016,** *18* (9), 1239-50.
52. Lotfabad E M, Ding J, Cui K, et al. High-density sodium and lithium ion battery anodes from banana peels[J]. ACS nano, 2014, 8(7): 7115-7129.

53. Memarzadeh Lotfabad, E.; Kalisvaart, P.; Kohandehghan, A.; Karpuzov, D.; Mitlin, D., Origin of non-SEI related coulombic efficiency loss in carbons tested against Na and Li. *J. Mater. Chem. A* **2014,** *2* (46), 19685-19695.
54. Sun, N.; Liu, H.; Xu, B., Facile synthesis of high performance hard carbon anode materials for sodium ion batteries. *Journal of Materials Chemistry A* **2015,** *3* (41), 20560-20566.
55. Zhang, C.; Xie, Z.; Yang, W.; Liang, Y.; Meng, D.; He, X.; Liang, P.; Zhang, Z., NiCo2O4/biomass-derived carbon composites as anode for high-performance lithium ion batteries. *Journal of Power Sources* **2020,** *451*, 227761.
56. Wu, L.; Buchholz, D.; Vaalma, C.; Giffin, G. A.; Passerini, S., Apple-Biowaste-Derived Hard Carbon as a Powerful Anode Material for Na-Ion Batteries. *ChemElectroChem* **2016,** *3* (2), 292-298.
57. Hao, J.; Wang, Y.; Chi, C.; Wang, J.; Guo, Q.; Yang, Y.; Li, Y.; Liu, X.; Zhao, J., Enhanced storage capability by biomass-derived porous carbon for lithium-ion and sodium-ion battery anodes. *Sustainable Energy & Fuels* **2018,** *2* (10), 2358-2365.
58. Kim, N. R.; Yun, Y. S.; Song, M. Y.; Hong, S. J.; Kang, M.; Leal, C.; Park, Y. W.; Jin, H. J., Citrus-Peel-Derived, Nanoporous Carbon Nanosheets Containing Redox-Active Heteroatoms for Sodium-Ion Storage. *ACS applied materials & interfaces* **2016,** *8* (5), 3175-81.
59. Hao, R.; Yang, Y.; Wang, H.; Jia, B.; Ma, G.; Yu, D.; Guo, L.; Yang, S., Direct chitin conversion to N-doped amorphous carbon nanofibers for high-performing full sodium-ion batteries. *Nano Energy* **2018,** *45*, 220-228.
60. Raj K, A.; Panda, M. R.; Dutta, D. P.; Mitra, S., Bio-derived mesoporous disordered carbon: An excellent anode in sodium-ion battery and full-cell lab prototype. *Carbon* **2019,** *143*, 402-412.
61. Xu, S.-D.; Zhao, Y.; Liu, S.; Ren, X.; Chen, L.; Shi, W.; Wang, X.; Zhang, D., Curly hard carbon derived from pistachio shells as high-performance anode materials for sodium-ion batteries. *Journal of Materials Science* **2018,** *53* (17), 12334-12351.
62. Hwang, Y. J.; Jeong, S. K.; Shin, J. S.; Nahm, K. S.; Stephan, A. M., High capacity disordered carbons obtained from coconut shells as anode materials for lithium batteries. *Journal of Alloys and Compounds* **2008,** *448* (1-2), 141-147.
63. Tian, W.; Wang, L.; Huo, K.; He, X., Red phosphorus filled biomass carbon as high-capacity and long-life anode for sodium-ion batteries. *Journal of Power Sources* **2019,** *430*, 60-66.
64. Chen, S.; Yang, H.; Chen, Q.; Liu, L.; Hou, X.; Luo, L.; Lin, C.; Li, C.; Chen, Y., Synthesis of BCN nanoribbons from coconut shells using as high-performance anode materials for lithium-ion batteries. *Electrochimica Acta* **2020,** *346*, 136239.
65. Lv, W.; Wen, F.; Xiang, J.; Zhao, J.; Li, L.; Wang, L.; Liu, Z.; Tian, Y., Peanut shell derived hard carbon as ultralong cycling anodes for lithium and sodium batteries. *Electrochimica Acta* **2015,** *176*, 533-541.
66. Wang, H.; Yu, W.; Shi, J.; Mao, N.; Chen, S.; Liu, W., Biomass derived hierarchical porous carbons as high-performance anodes for sodium-ion batteries. *Electrochimica Acta* **2016,** *188*, 103-110.
67. Wang, L.; Schnepp, Z.; Titirici, M. M., Rice husk-derived carbon anodes for lithium ion batteries. *Journal of Materials Chemistry A* **2013,** *1* (17), 5269.
68. Luo, D.; Han, P.; Shi, L.; Huang, J.; Yu, J.; Lin, Y.; Du, J.; Yang, B.; Li, C.; Zhu, C.; Xu, J., Biomass-derived nitrogen/oxygen co-doped hierarchical porous carbon with a large specific surface area for ultrafast and long-life sodium-ion batteries. *Applied Surface Science* **2018,** *462*, 713-719.
69. Zhu, Y.; Chen, M.; Li, Q.; Yuan, C.; Wang, C., A porous biomass-derived anode for high-performance sodium-ion batteries. *Carbon* **2018,** *129*, 695-701.
70. Zhang, F.; Wang, K.-X.; Li, G.-D.; Chen, J.-S., Hierarchical porous carbon derived from rice straw for lithium ion batteries with high-rate performance. *Electrochemistry Communications* **2009,** *11* (1), 130-133.
71. Chen, L.; Zhang, Y.; Lin, C.; Yang, W.; Meng, Y.; Guo, Y.; Li, M.; Xiao, D., Hierarchically porous nitrogen-rich carbon derived from wheat straw as an ultra-high-rate anode for lithium ion batteries. *J. Mater. Chem. A* **2014,** *2* (25), 9684-9690.

72. Li, Y.; Li, C.; Qi, H.; Yu, K.; Li, X., Formation mechanism and characterization of porous biomass carbon for excellent performance lithium-ion batteries. *RSC Advances* **2018,** *8* (23), 12666-12671.
73. Xiong, J.; Pan, Q.; Zheng, F.; Xiong, X.; Yang, C.; Hu, D.; Huang, C., N/S Co-doped Carbon Derived From Cotton as High Performance Anode Materials for Lithium Ion Batteries. *Front Chem* **2018,** *6*, 78.
74. Sankar, S.; Saravanan, S.; Ahmed, A. T. A.; Inamdar, A. I.; Im, H.; Lee, S.; Kim, D. Y., Spherical activated-carbon nanoparticles derived from biomass green tea wastes for anode material of lithium-ion battery. *Materials Letters* **2019,** *240*, 189-192.
75. Chen, K.; Li, G.; Wang, Y.; Chen, W.; Mi, L., High loading FeS2 nanoparticles anchored on biomass-derived carbon tube as low cost and long cycle anode for sodium-ion batteries. *Green Energy & Environment* **2020,** *5* (1), 50-58.
76. Zhu, Y.; Huang, Y.; Chen, C.; Wang, M.; Liu, P., Phosphorus-doped porous biomass carbon with ultra-stable performance in sodium storage and lithium storage. *Electrochimica Acta* **2019,** *321*, 134698.
77. Dou, Y.; Liu, X.; Yu, K.; Wang, X.; Liu, W.; Liang, J.; Liang, C., Biomass porous carbon derived from jute fiber as anode materials for lithium-ion batteries. *Diamond and Related Materials* **2019,** *98*, 107514.
78. Wang, C.; Huang, J.; Li, J.; Cao, L.; Chen, Q.; Qian, C.; Chen, S., Revealing the Effect of Nanopores in Biomass‐Derived Carbon on its Sodium‐Ion Storage Behavior. *ChemElectroChem* **2020,** *7* (1), 201-211.
79. Wang, X.; Zhao, J.; Yao, D.; Xu, Y.; Xu, P.; Chen, Y.; Chen, Y.; Zhu, K.; Cheng, K.; Ye, K.; Yan, J.; Cao, D.; Wang, G., Bio-derived hierarchically porous heteroatoms doped-carbon as anode for high performance potassium-ion batteries. *Journal of Electroanalytical Chemistry* **2020,** *871*, 114272.
80. Qiu, D.; Kang, C.; Li, M.; Wei, J.; Hou, Z.; Wang, F.; Yang, R., Biomass-derived mesopore-dominant hierarchical porous carbon enabling ultra-efficient lithium ion storage. *Carbon* **2020,** *162*, 595-603.
81. Chen, Y.; Liu, H.; Jiang, B.; Zhao, Y.; Meng, X.; Ma, T., Hierarchical porous architectures derived from low-cost biomass equisetum arvense as a promising anode material for lithium-ion batteries. *Journal of Molecular Structure* **2020,** *1221*, 128794.
82. Zhang, Y.-C.; You, Y.; Xin, S.; Yin, Y.-X.; Zhang, J.; Wang, P.; Zheng, X.-s.; Cao, F.-F.; Guo, Y.-G., Rice husk-derived hierarchical silicon/nitrogen-doped carbon/carbon nanotube spheres as low-cost and high-capacity anodes for lithium-ion batteries. *Nano Energy* **2016,** *25*, 120-127.
83. Zhou, D.; Shen, D.; Lu, W.; Song, T.; Wang, M.; Feng, H.; Shentu, J.; Long, Y., Production of 5-Hydroxymethylfurfural from Chitin Biomass: A Review. *Molecules* **2020,** *25* (3).
84. Elizabeth, I.; Singh, B. P.; Trikha, S.; Gopukumar, S., Bio-derived hierarchically macro-meso-micro porous carbon anode for lithium/sodium ion batteries. *Journal of Power Sources* **2016,** *329*, 412-421.
85. Gao, F.; Geng, C.; Xiao, N.; Qu, J.; Qiu, J., Hierarchical porous carbon sheets derived from biomass containing an activation agent and in-built template for lithium ion batteries. *Carbon* **2018,** *139*, 1085-1092.
86. Dong, H.; Zhang, H.; Xu, Y.; Zhao, C., Facile synthesis of α-Fe2O3 nanoparticles on porous human hair-derived carbon as improved anode materials for lithium ion batteries. *Journal of Power Sources* **2015,** *300*, 104-111.
87. Ou, J.; Zhang, Y.; Chen, L.; Zhao, Q.; Meng, Y.; Guo, Y.; Xiao, D., Nitrogen-rich porous carbon derived from biomass as a high performance anode material for lithium ion batteries. *Journal of Materials Chemistry A* **2015,** *3* (12), 6534-6541.
88. Wang Y, Zhang L, Wang H, et al. Sustainable synthesis of Penicillium-derived highly conductive carbon film as superior binder-free electrode of lithium ion batteries[J]. Journal of Solid State Electrochemistry, 2014, 18(11): 3209-3214.
89. Cheng, J.; Zhang, G.; Wang, P.; Wang, C. Y.; Yin, Y. X.; Li, Y. K.; Cao, F. F.; Guo, Y. G., Confined Red Phosphorus in Edible Fungus Slag-Derived Porous Carbon as an Improved Anode Material in Sodium-Ion Batteries. *ACS applied materials & interfaces* **2019,** *11* (51), 47948-47955.
90. Tang, J.; Etacheri, V.; Pol, V. G., Wild Fungus Derived Carbon Fibers and Hybrids as Anodes for Lithium-Ion Batteries. *ACS Sustainable Chemistry & Engineering* **2016,** *4* (5), 2624-2631.

91. Li, Q.; Liu, D.; Jia, Z.; Csetenyi, L.; Gadd, G. M., Fungal Biomineralization of Manganese as a Novel Source of Electrochemical Materials. *Curr Biol* **2016,** *26* (7), 950-5.
92. Shan, Y.; Li, Y.; Pang, H., Applications of Tin Sulfide‐Based Materials in Lithium‐Ion Batteries and Sodium‐Ion Batteries. *Advanced Functional Materials* **2020,** *30* (23), 2001298.
93. Chae, S.; Choi, S. H.; Kim, N.; Sung, J.; Cho, J., Integration of Graphite and Silicon Anodes for the Commercialization of High-Energy Lithium-Ion Batteries. *Angewandte Chemie* **2020,** *59* (1), 110-135.
94. Hou, G.; Cheng, B.; Yang, Y.; Du, Y.; Zhang, Y.; Li, B.; He, J.; Zhou, Y.; Yi, D.; Zhao, N.; Bando, Y.; Golberg, D.; Yao, J.; Wang, X.; Yuan, F., Multiscale Buffering Engineering in Silicon-Carbon Anode for Ultrastable Li-Ion Storage. *ACS nano* **2019,** *13* (9), 10179-10190.
95. Zhang, X.; Wang, D.; Qiu, X.; Ma, Y.; Kong, D.; Mullen, K.; Li, X.; Zhi, L., Stable high-capacity and high-rate silicon-based lithium battery anodes upon two-dimensional covalent encapsulation. *Nature communications* **2020,** *11* (1), 3826.
96. Niu, F.; Yang, J.; Wang, N.; Zhang, D.; Fan, W.; Yang, J.; Qian, Y., MoSe2-Covered N,P-Doped Carbon Nanosheets as a Long-Life and High-Rate Anode Material for Sodium-Ion Batteries. *Advanced Functional Materials* **2017,** *27* (23), 1700522.
97. Yan, J.; Wang, Q.; Wei, T.; Fan, Z., Recent Advances in Design and Fabrication of Electrochemical Supercapacitors with High Energy Densities. *Advanced Energy Materials* **2014,** *4* (4), 1300816.
98. Wang, J.; Kaskel, S., KOH activation of carbon-based materials for energy storage. *Journal of Materials Chemistry* **2012,** *22* (45), 23710.
99. Cui, J.; Cheng, F.; Lin, J.; Yang, J.; Jiang, K.; Wen, Z.; Sun, J., High surface area C/SiO2 composites from rice husks as a high-performance anode for lithium ion batteries. *Powder Technology* **2017,** *311*, 1-8.
100. Wu H, Amine K, Lu J. Cathode materials for lithium ion batteries: U.S. Patent 10,833,321[P]. 2020-11-10.
101. Hernandez-Rentero, C.; Marangon, V.; Olivares-Marin, M.; Gomez-Serrano, V.; Caballero, A.; Morales, J.; Hassoun, J., Alternative lithium-ion battery using biomass-derived carbons as environmentally sustainable anode. *Journal of colloid and interface science* **2020,** *573*, 396-408.
102. Wang, X.; Sun, G.; Routh, P.; Kim, D. H.; Huang, W.; Chen, P., Heteroatom-doped graphene materials: syntheses, properties and applications. *Chemical Society reviews* **2014,** *43* (20), 7067-98.
103. Lin, C.; Song, S.; Lai, M. O.; Lu, L., Li 3.9 Cu 0.1 Ti 5 O 12 /CNTs composite for the anode of high-power lithium-ion batteries: Intrinsic and extrinsic effects. *Electrochimica Acta* **2014,** *143*, 29-35.
104. Lafkioti, M.; Krauss, B.; Lohmann, T.; Zschieschang, U.; Klauk, H.; Klitzing, K. V.; Smet, J. H., Graphene on a hydrophobic substrate: doping reduction and hysteresis suppression under ambient conditions. *Nano letters* **2010,** *10* (4), 1149-53.
105. Guo, S.; Chen, Y.; Shi, L.; Dong, Y.; Ma, J.; Chen, X.; Song, H., Nitrogen-doped biomass-based ultra-thin carbon nanosheets with interconnected framework for High-Performance Lithium-Ion Batteries. *Applied Surface Science* **2018,** *437*, 136-143.
106. Zheng, F.; Liu, D.; Xia, G.; Yang, Y.; Liu, T.; Wu, M.; Chen, Q., Biomass waste inspired nitrogen-doped porous carbon materials as high-performance anode for lithium-ion batteries. *Journal of Alloys and Compounds* **2017,** *693*, 1197-1204.
107. Hao E, Liu W, Liu S, et al. Rich sulfur doped porous carbon materials derived from ginkgo leaves for multiple electrochemical energy storage devices[J]. Journal of materials chemistry a, 2017, 5(5): 2204-2214.
108. Li, R.; Huang, J.; Li, J.; Cao, L.; Zhong, X.; Yu, A.; Lu, G., Nitrogen-doped porous hard carbons derived from shaddock peel for high-capacity lithium-ion battery anodes. *Journal of Electroanalytical Chemistry* **2020,** *862*, 114044.
109. Qiu, Z.; Lin, Y.; Xin, H.; Han, P.; Li, D.; Yang, B.; Li, P.; Ullah, S.; Fan, H.; Zhu, C.; Xu, J., Ultrahigh level nitrogen/sulfur co-doped carbon as high performance anode materials for lithium-ion batteries. *Carbon* **2018,** *126*, 85-92.

110. Shi, S.; Li, Z.; Sun, Y.; Wang, B.; Liu, Q.; Hou, Y.; Huang, S.; Huang, J.; Zhao, Y., A covalent heterostructure of monodisperse Ni2P immobilized on N, P-co-doped carbon nanosheets for high performance sodium/lithium storage. *Nano Energy* **2018,** *48*, 510-517.
111. Wu, Y.; Zhu, C.; Shu, L.; Duan, J.; Wei, D.; Xu, J.; Zhu, Z.; Li, L.; Peng, Z.; Chen, Z., Co9S8 confined in bifunctional N/S co-doped carbon/carbon with high electrochemical performance for lithium-ion batteries. *Applied Surface Science* **2019,** *489*, 528-537.
112. Ou, J.; Yang, L.; Zhang, Z.; Xi, X., Honeysuckle-derived hierarchical porous nitrogen, sulfur, dual-doped carbon for ultra-high rate lithium ion battery anodes. *Journal of Power Sources* **2016,** *333*, 193-202.
113. Zhao, H.; Gao, Y.; Wang, J.; Chen, C.; Chen, D.; Wang, C.; Ciucci, F., Egg yolk-derived phosphorus and nitrogen dual doped nano carbon capsules for high-performance lithium ion batteries. *Materials Letters* **2016,** *167*, 93-97.
114. Lu, M.; Yu, W.; Shi, J.; Liu, W.; Chen, S.; Wang, X.; Wang, H., Self-doped carbon architectures with heteroatoms containing nitrogen, oxygen and sulfur as high-performance anodes for lithium- and sodium-ion batteries. *Electrochimica Acta* **2017,** *251*, 396-406.
115. Li, K.; Zhang, Y.; Sun, Y.; Xu, Y.; Zhang, H.; Ye, P.; Zheng, M.; Zhou, N.; Wang, D., Template-free synthesis of biomass-derived carbon coated Li4Ti5O12 microspheres as high performance anodes for lithium-ion batteries. *Applied Surface Science* **2018,** *459*, 572-582.
116. Chen, Y.; Xu, Y.; Li, Z.; Zhang, W.; Zheng, M.; Zhang, H., Biomass-mediated synthesis of carbon-supported ZnMn2O4 nanoparticles as high-performance anode materials for lithium-ion batteries. *Colloids and Surfaces A: Physicochemical and Engineering Aspects* **2020,** *600*, 124941.
117. Xu, X.; Meng, Z.; Zhu, X.; Zhang, S.; Han, W.-Q., Biomass carbon composited FeS 2 as cathode materials for high-rate rechargeable lithium-ion battery. *Journal of Power Sources* **2018,** *380*, 12-17.
118. Lin, J.; Cui, J.; Cheng, F.; Cui, Y.; Sun, H.; Sun, J., Self-assembled porous microsized composite of nano-Co1−xS/biomass derived activated carbon by a facile solvothermal method as anode material of lithium ion battery. *Journal of Alloys and Compounds* **2017,** *695*, 2173-2179.
119. Wu, J.; Zuo, L.; Song, Y.; Chen, Y.; Zhou, R.; Chen, S.; Wang, L., Preparation of biomass-derived hierarchically porous carbon/Co 3 O 4 nanocomposites as anode materials for lithium-ion batteries. *Journal of Alloys and Compounds* **2016,** *656*, 745-752.
120. Song, D.; Park, J.; Kim, K.; Lee, L. S.; Seo, J. Y.; Oh, Y.-K.; Kim, Y.-J.; Ryou, M.-H.; Lee, Y. M.; Lee, K., Recycling oil-extracted microalgal biomass residues into nano/micro hierarchical Sn/C composite anode materials for lithium-ion batteries. *Electrochimica Acta* **2017,** *250*, 59-67.
121. Li, X.; Yan, P.; Xiao, X.; Woo, J. H.; Wang, C.; Liu, J.; Zhang, J.-G., Design of porous Si/C–graphite electrodes with long cycle stability and controlled swelling. *Energy & Environmental Science* **2017,** *10* (6), 1427-1434.
122. Parekh, M. H.; Sediako, A. D.; Naseri, A.; Thomson, M. J.; Pol, V. G., In Situ Mechanistic Elucidation of Superior Si‐C‐Graphite Li‐Ion Battery Anode Formation with Thermal Safety Aspects. *Advanced Energy Materials* **2019,** *10* (2), 1902799.
123. Lv, X.; Wei, W.; Huang, B.; Dai, Y., Achieving high energy density for lithium-ion battery anodes by Si/C nanostructure design. *Journal of Materials Chemistry A* **2019,** *7* (5), 2165-2171.
124. Li, W.; Tang, Y.; Kang, W.; Zhang, Z.; Yang, X.; Zhu, Y.; Zhang, W.; Lee, C. S., Core-shell Si/C nanospheres embedded in bubble sheet-like carbon film with enhanced performance as lithium ion battery anodes. *Small* **2015,** *11* (11), 1345-51.
125. Liu, J.; Kopold, P.; van Aken, P. A.; Maier, J.; Yu, Y., Energy Storage Materials from Nature through Nanotechnology: A Sustainable Route from Reed Plants to a Silicon Anode for Lithium-Ion Batteries. *Angewandte Chemie* **2015,** *54* (33), 9632-6.
126. Zhang, C.; Cai, X.; Chen, W.; Yang, S.; Xu, D.; Fang, Y.; Yu, X., 3D Porous Silicon/N-Doped Carbon Composite Derived from Bamboo Charcoal as High-Performance Anode Material for Lithium-Ion Batteries. *ACS Sustainable Chemistry & Engineering* **2018,** *6* (8), 9930-9939.

127. Xu, Q.; Sun, J.-K.; Yin, Y.-X.; Guo, Y.-G., Facile Synthesis of Blocky SiOx/C with Graphite-Like Structure for High-Performance Lithium-Ion Battery Anodes. *Advanced Functional Materials* **2018,** *28* (8), 1705235.

128. Liu, Z.; Guan, D.; Yu, Q.; Xu, L.; Zhuang, Z.; Zhu, T.; Zhao, D.; Zhou, L.; Mai, L., Monodisperse and homogeneous SiO /C microspheres: A promising high-capacity and durable anode material for lithium-ion batteries. *Energy Storage Materials* **2018,** *13*, 112-118.
129. Ju, Y.; Tang, J. A.; Zhu, K.; Meng, Y.; Wang, C.; Chen, G.; Wei, Y.; Gao, Y., SiO x /C composite from rice husks as an anode material for lithium-ion batteries. *Electrochimica Acta* **2016,** *191*, 411-416.
130. Cui, J.; Cheng, F.; Lin, J.; Yang, J.; Jiang, K.; Wen, Z.; Sun, J., High surface area C/SiO 2 composites from rice husks as a high-performance anode for lithium ion batteries. *Powder Technology* **2017,** *311*, 1-8.
131. Guo, X.; Zhang, Y.-Z.; Zhang, F.; Li, Q.; Anjum, D. H.; Liang, H.; Liu, Y.; Liu, C.-s.; Alshareef, Husam N.; Pang, H., A novel strategy for the synthesis of highly stable ternary SiOx composites for Li-ion-battery anodes. *Journal of Materials Chemistry A* **2019,** *7* (26), 15969-15974.
132. Huang, X.; Liu, D.; Guo, X.; Sui, X.; Qu, D.; Chen, J., Phosphorus/Carbon Composite Anode for Potassium-Ion Batteries: Insights into High Initial Coulombic Efficiency and Superior Cyclic Performance. *ACS Sustainable Chemistry & Engineering* **2018,** *6* (12), 16308-16314.
133. He, P.; Fang, Y.; Yu, X. Y.; Lou, X. W. D., Hierarchical Nanotubes Constructed by Carbon-Coated Ultrathin SnS Nanosheets for Fast Capacitive Sodium Storage. *Angewandte Chemie* **2017,** *56* (40), 12202-12205.
134. Zhang, J.; Shin, H.; Lu, W., Highly ambient-stable few-layer black phosphorene by pulsed laser exfoliation and HEMM. *Chemical communications* **2019,** *55* (18), 2601-2604.
135. Wang, K.; Xu, Y.; Li, Y.; Dravid, V.; Wu, J.; Huang, Y., Sodium storage in hard carbon with curved graphene platelets as the basic structural units. *Journal of Materials Chemistry A* **2019,** *7* (7), 3327-3335.
136. Hu, H.-Y.; Xiao, Y.; Ling, W.; Wu, Y.-B.; Wang, P.; Tan, S.-J.; Xu, Y.-S.; Guo, Y.-J.; Chen, W.-P.; Tang, R.-R.; Zeng, X.-X.; Yin, Y.-X.; Wu, X.-W., A Stable Biomass‐Derived Hard Carbon Anode for High‐Performance Sodium‐Ion Full Battery. *Energy Technology* **2020,** *9* (1), 2000730.
137. Yin, Y.; Zhang, Y.; Liu, N.; Sun, B.; Zhang, N., Biomass-Derived P/N-Co-Doped Carbon Nanosheets Encapsulate Cu3P Nanoparticles as High-Performance Anode Materials for Sodium-Ion Batteries. *Front Chem* **2020,** *8*, 316.
138. Susanti, R. F.; Alvin, S.; Kim, J., Toward high-performance hard carbon as an anode for sodium-ion batteries: Demineralization of biomass as a critical step. *Journal of Industrial and Engineering Chemistry* **2020,** *91*, 317-329.
139. Wang, J.; Yan, L.; Ren, Q.; Fan, L.; Zhang, F.; Shi, Z., Facile hydrothermal treatment route of reed straw-derived hard carbon for high performance sodium ion battery. *Electrochimica Acta* **2018,** *291*, 188-196.
140. Kim, K.; Lim, D. G.; Han, C. W.; Osswald, S.; Ortalan, V.; Youngblood, J. P.; Pol, V. G., Tailored Carbon Anodes Derived from Biomass for Sodium-Ion Storage. *ACS Sustainable Chemistry & Engineering* **2017,** *5* (10), 8720-8728.
141. Hao, E.; Liu, W.; Liu, S.; Zhang, Y.; Wang, H.; Chen, S.; Cheng, F.; Zhao, S.; Yang, H., Rich sulfur doped porous carbon materials derived from ginkgo leaves for multiple electrochemical energy storage devices. *Journal of Materials Chemistry A* **2017,** *5* (5), 2204-2214.
142. Wang, P.; Yang, B.; Zhang, G.; Zhang, L.; Jiao, H.; Chen, J.; Yan, X., Three-dimensional carbon framework as a promising anode material for high performance sodium ion storage devices. *Chemical Engineering Journal* **2018,** *353*, 453-459.
143. Yan, D.; Yu, C.; Zhang, X.; Qin, W.; Lu, T.; Hu, B.; Li, H.; Pan, L., Nitrogen-doped carbon microspheres derived from oatmeal as high capacity and superior long life anode material for sodium ion battery. *Electrochimica Acta* **2016,** *191*, 385-391.
144. Wang, P.; Qiao, B.; Du, Y.; Li, Y.; Zhou, X.; Dai, Z.; Bao, J., Fluorine-Doped Carbon Particles Derived from Lotus Petioles as High-Performance Anode Materials for Sodium-Ion Batteries. *The Journal of Physical Chemistry C* **2015,** *119* (37), 21336-21344.

145. Li, W.; Zhou, M.; Li, H.; Wang, K.; Cheng, S.; Jiang, K., A high performance sulfur-doped disordered carbon anode for sodium ion batteries. *Energy & Environmental Science* **2015,** *8* (10), 2916-2921.
146. Chen H, Zhang W, Tang X Q, et al. First principles study of P-doped borophene as anode materials for lithium ion batteries[J]. Applied Surface Science, 2018, 427: 198-205.
147. Guo, L.; An, Y.; Fei, H.; Feng, J.; Xiong, S.; Ci, L., Self-templated biomass-derived nitrogen-doped porous carbons as high-performance anodes for sodium ion batteries. *Materials Technology* **2017,** *32* (10), 592-597.
148. Zhao, G.; Yu, D.; Zhang, H.; Sun, F.; Li, J.; Zhu, L.; Sun, L.; Yu, M.; Besenbacher, F.; Sun, Y., Sulphur-doped carbon nanosheets derived from biomass as high-performance anode materials for sodium-ion batteries. *Nano Energy* **2020,** *67*, 104219.
149. Hu, Y.; Shen, L.; Wei, X.; Long, Z.; Guo, X.; Qiu, X., One‐Pot Synthesis of Novel B, N Co‐Doped Carbon Materials for High‐Performance Sodium‐Ion Batteries. *ChemistrySelect* **2019,** *4* (21), 6445-6450.
150. Zhu, Y.; Huang, Y.; Wang, M.; Chen, C., Nitrogen and phosphorus co-doped 3D hierarchical porous carbon network with highly-reversible performance in sodium storage. *Ceramics International* **2019,** *45* (18), 24500-24507.
151. Ru H, Xiang K, Zhou W, et al. Bean-dreg-derived carbon materials used as superior anode material for lithium-ion batteries[J]. Electrochimica Acta, 2016, 222: 551-560.
152. Li, D.; Sun, Y.; Chen, S.; Yao, J.; Zhang, Y.; Xia, Y.; Yang, D., Highly Porous FeS/Carbon Fibers Derived from Fe-Carrageenan Biomass: High-capacity and Durable Anodes for Sodium-Ion Batteries. *ACS applied materials & interfaces* **2018,** *10* (20), 17175-17182.
153. Wu, H.; Li, X.; Chen, L.; Dan, Y., Facile Synthesis of Hierarchical Iron Phosphide/Biomass Carbon Composites for Binder-Free Sodium-Ion Batteries. *Batteries & Supercaps* **2019,** *2* (2), 144-152.
154. Dutta, D. P., Composites of Sb_2O_4 and Biomass‐Derived Mesoporous Disordered Carbon as Versatile Anodes for Sodium‐Ion Batteries. *ChemistrySelect* **2020,** *5* (6), 1846-1857.

155. Wang, J.; Zhang, G.; Liu, Z.; Li, H.; Liu, Y.; Wang, Z.; Li, X.; Shih, K.; Mai, L., Li3V(MoO4)3 as a novel electrode material with good lithium storage properties and improved initial coulombic efficiency. *Nano Energy* **2018,** *44*, 272-278.
156. Chen, S.; Fan, L.; Xu, L.; Liu, Q.; Qin, Y.; Lu, B., 100 K cycles: Core-shell H-FeS@C based lithium-ion battery anode. *Energy Storage Materials* **2017,** *8*, 20-27.
157. Zhang, X.; Cheng, X.; Zhang, Q., Nanostructured energy materials for electrochemical energy conversion and storage: A review. *Journal of Energy Chemistry* **2016,** *25* (6), 967-984.
158. Fan, L.; Chen, S.; Ma, R.; Wang, J.; Wang, L.; Zhang, Q.; Zhang, E.; Liu, Z.; Lu, B., Ultrastable Potassium Storage Performance Realized by Highly Effective Solid Electrolyte Interphase Layer. *Small* **2018,** *14* (30), e1801806.
159. Cao, W.; Zhang, E.; Wang, J.; Liu, Z.; Ge, J.; Yu, X.; Yang, H.; Lu, B., Potato derived biomass porous carbon as anode for potassium ion batteries. *Electrochimica Acta* **2019,** *293*, 364-370.
160. Yang, M.; Dai, J.; He, M.; Duan, T.; Yao, W., Biomass-derived carbon from Ganoderma lucidum spore as a promising anode material for rapid potassium-ion storage. *Journal of colloid and interface science* **2020,** *567*, 256-263.
161. Gao, C.; Wang, Q.; Luo, S.; Wang, Z.; Zhang, Y.; Liu, Y.; Hao, A.; Guo, R., High performance potassium-ion battery anode based on biomorphic N-doped carbon derived from walnut septum. *Journal of Power Sources* **2019,** *415*, 165-171.
162. Wu, Z.; Wang, L.; Huang, J.; Zou, J.; Chen, S.; Cheng, H.; Jiang, C.; Gao, P.; Niu, X., Loofah-derived carbon as an anode material for potassium ion and lithium ion batteries. *Electrochimica Acta* **2019,** *306*, 446-453.
163. Li Q, Yi T, Wang X, et al. In-situ visualization of lithium plating in all-solid-state lithium-metal battery[J]. Nano Energy, 2019, 63: 103895.

164. Schnell J, Günther T, Knoche T, et al. All-solid-state lithium-ion and lithium metal batteries–paving the way to large-scale production[J]. Journal of Power Sources, 2018, 382: 160-175.
165. Wang C, Wang T, Wang L, et al. Differentiated lithium salt design for multilayered PEO electrolyte enables a high‐voltage solid‐state lithium metal battery[J]. Advanced Science, 2019, 6(22): 1901036.
166. Zhou, F.; Li, Z.; Lu, Y. Y.; Shen, B.; Guan, Y.; Wang, X. X.; Yin, Y. C.; Zhu, B. S.; Lu, L. L.; Ni, Y.; Cui, Y.; Yao, H. B.; Yu, S. H., Diatomite derived hierarchical hybrid anode for high performance all-solid-state lithium metal batteries. *Nature communications* **2019,** *10* (1), 2482.